

# Design and Fabrication of Solar PV Cleaning Robot

*by* Swasti Agarwal

---

**Submission date:** 03-Aug-2022 09:20AM (UTC+0530)

**Submission ID:** 1878306738

**File name:** G5\_-\_report\_edited-pages.pdf (19.14M)

**Word count:** 13846

**Character count:** 64907

## CHAPTER 1

### INTRODUCTION

Energy-related aspects are gaining a lot of importance in today's world and play an essential role in the basic functioning of modern society. Based on the source it is derived from, energy resources can be categorized as conventional and non-conventional [1]. Conventional energy is derived from resources that are non-renewable that means once a sample of conventional energy resource is used up, it cannot be used again whereas non-conventional energy is derived from resources that are renewable like solar energy.

Due to the continuous depletion in the available conventional energy resources like coal, oil etc, and their harmful effect on the environment, the attention is steered towards utilizing and developing renewable and sustainable energy sources. Non-conventional energy resources are much more sustainable and their impact on the environment is less hazardous [3]. This growing interest in renewable energy has resulted in a significant expansion of the solar photovoltaic sector as **solar energy is the most common and cleanest source of energy** with abundant availability.<sup>3</sup>

Solar energy is the energy consisting of light and heat that is harnessed with the help of solar heating, solar thermal energy, photovoltaics, artificial photosynthesis and so on [11]. It one of the most widely available and fairly distributed resource on the planet but it is hardly utilised [9]. It is also the cleanest source of power available known to humans till date. PV systems ensure the generation of energy with low environmental impact while ensuring significant margins of improvement [4].

The world receives enough solar radiation to fulfill the demands of the solar power systems. Earth receives approximately about 174 PW <sup>11</sup> of energy in the form of solar power <sup>11</sup> out of which 31% is reflected back to space and is absorbed by clouds <sup>66</sup> [5]. The Global Horizontal Irradiation (GHI) in different parts of the world is shown in Figure 1.1.

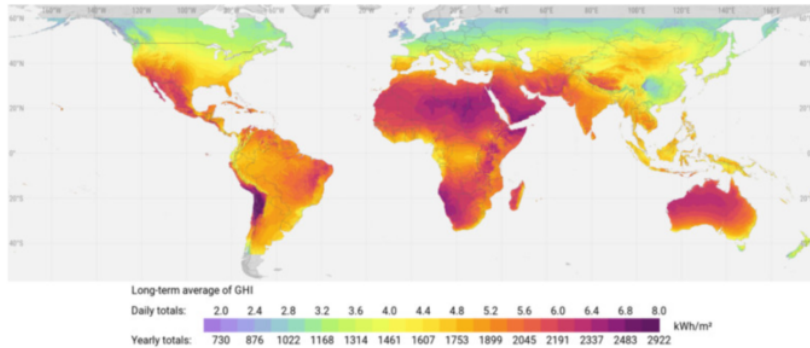


Figure 1.1: Global Horizontal Irradiation Across Globe [17]

Around 11.8% of power generated in India is through solar power that reaches to about 53.997 GW (as of 31st March 2021). As the country is planning to establish a greater number of solar power generation plants, it has resulted in creating more opportunities to build sustainable and efficient solar power plants [7]. The efficiency of solar panels is generally around 15-20% because some of the photons are reflected back or the energy is converted into heat instead of producing electric current. The efficiency decreases by a considerable amount due the accumulation of dust on the panels [16]. Considering this, it is essential to maintain the solar power output in optimum value by cleaning the panels regularly [10].

## 1.1 Literature survey

In order to build an effective cleaning robot for the solar panels, the knowledge of solar power generation and the factors affecting the performance of solar power plants is required. Hence, the study of various research papers on this subject provides an idea about the existing situation in the field of solar energy and cleaning methods. The literature review has been sectionalised as follows.

### 1.1.1 Parameters Affecting Performance of PV Panels

Surajit Mondal et al. state that there are certain external parameters that affect the output of PV panels such as dust accumulation on the panels. Various methods are employed in order to minimize the effect of dust on the panel that result in reduction of

adhesive bonds between the pollutants with the help of repulsion by electrostatic means. The major methods include electrostatic biasing, standing wave and multiphase electric curtain. It consists of rows of conducting, parallel and transparent electrodes that are sandwiched between two dielectric layers that are made to be in contact with the solar photovoltaic panel layer. The electrodes are activated with the application of low-frequency, high-voltage pulses and by Coulomb force, the dust particles are removed. It depends on the distribution of electric field and charge acquired by dust particles during the operation [1].

Benatia et al. demonstrate that there are many experiments that were carried out in the desert environment with high irradiance and with the introduction of various types of dust. The performance of the solar panels was determined in the presence of dust and readings were recorded after cleaning the surface in order to compare both the readings. The conclusion has been drawn out that there is a 50% reduction in the output power [2].

### 1.1.2 Development of Cleaning Robot

Kiran M R and Rekha G Padaki project a model of a cleaning robot runs on a self-cleaning mechanism that involves mechanical and electrical elements. A DC motor is used under the mechanical element to control the robot that moves on the panel upwards and downwards. The electrical element consists of a software program that includes two elements and they operate and control the structures of the self cleaning robot. The software program includes essential programs and an interrupt process. The output strength of the panel is measured before and after cleaning in order to analyze the efficiency [3].

S. K. Thomas et al. conducted experiments on a <sup>3</sup> solar panel automated cleaning (SPAC) system that uses soft yet powerful nylon brushes to clean the panels and also has two squeegees on either side of the brush to wipe out water. The system is retrofitted directly on to the panels in solar power plant, commercial, residential sectors. This system is vibration free, it is capable of cleaning multiple rows and the water is also reused. The intent of the project is to improve the solar panel efficiency by removing all kinds of dust particles [4].

A.Gheitasi et al. developed a low-cost automation device to preserve the output of solar panels connected to the array by offering on-demand cleaning. Wireless Sensor networks have been set up to collect data from individual panels. Monitoring details and knowledge patterns are then used to activate a robotic device to clean the surface of unclean panels [5].

M. A. Jaradat et al. show another model of robot using a portable robotic cleaning device that travels the whole panel length. To execute the robot control system an Arduino microcontroller is used. Initial robot testing has yielded favorable results and shows that a system like that is viable. Future design enhancements are discussed, in particular the various methods of transporting the robot from one panel to another. In conclusion, robotic cleaning solution is found to be practical and helps in maintaining the efficiency of the clean PV panel [6].

Q. Zhang et al. proposed a linear piezoelectric actuator based solar panel cleaning device to ensure that a solar panel performs at the best state of power generation using the solar panel in a dusty environment. A piezoelectric actuator is used to drive a wiper that moves linearly on a guide. The actuator drives a wiper to effectively wipe a layer of dust on the surface of the solar panel. The energy gain of the cleaning device, that is defined as the ratio of the increase in electric energy output of a solar panel caused by cleaning the piezoelectric actuator to energy consumption, is much higher than 1. It is advantageous to use a piezoelectric actuator due to its lightweight and compact structure feature[7].

T. Sorndach et al. present a solar panel cleaning robot that includes an omni wheel that allows the robot to rotate and move freely and avoid turning the robot while in operation. This research conceived and developed the robot's drive system for climbing the inclined and slippery solar panels. The robot was fitted with sensors and encoders to accurately monitor its travel, such as going through spaces between panels and halting at the ends of the panels. According to the tests conducted, the robot can travel on an inclined surface panel up to 10 degree angle elevation. Moving speed ranged from

0.16-0.34 m / s while going up and down the inclined panels due to sliding. Relative to the regular robot after 12 meters of cleaning space, the omni-wheel robot had an error of 0.3 per cent (similar to the standard robot) but saved around 64 per cent of the cleaning time by spinning instead of turning [8].

G. Aravind, G et al. implemented an autonomous system of vacuum cleaning to increase a solar panel's lifetime and efficiency. Two subsystems, including a Robotic Vacuum Cleaner and a Docking Station, are used to execute this system. To clear the dust from the solar panel, the Robotic Vacuum Cleaner uses a two-stage cleaning cycle. It's designed to operate on sloping and inclined surfaces. A control strategy is formulated, using an appropriate feedback mechanism, to navigate the robot in the required path. The robot's battery voltage is measured regularly, and if it reaches less than a specified level, it returns to the docking station and automatically repairs itself using the electricity from the solar panels. The robotic vacuum cleaner process has been checked and the related findings are provided. In Proteus' environment the DC charging circuit at the docking station is simulated and implemented in the hardware. A cost-effective and robust Robotic Vacuum Cleaner is designed and implemented that clean arrays of solar panels (with or without inclination) interlinked by rails and automatically recharges at a docking station [9].

Wallaaldin Eltayeb et al. developed a solar panel cleaning robot with sun tracking that cleans the panel using a rotary brush with water spray. Sun tracking mechanism is used to improve the efficiency of the solar panels. The robot frame is constructed using Aluminum due to its lightweight feature and resistance to corrosion. Sensors are used in the system to identify the presence of sunlight. A micro controller reacts to the sensor data by measuring output power from the solar panel and the cleaning mechanism becomes active only when the efficiency/output power is low. The robot is charged in standby mode. When the robot starts working, cleaning brushes rotate and move down vertically across the panel and once cleaning of the panel is complete, the cleaning brush stops rotating, moves up vertically and then moves horizontally to the next panel. This cycle continues until the end of the panel. The device then returns to the parking station located at the left side of the panel array for charging, while waiting for the activation

command. The robot can clean the surface using water and brush, and can also be used without water. A water pump is used that spreads water through the sprinkler on the panel surface [10].

### 1.1.3 Aspects of Controlling and Monitoring

Neha and S. Santosh Kumar implemented a Smart Solar panel cleaning device that focuses primarily on using the technologies of Internet of Things (IoT) is discussed. This allows for dust tracking capability, advanced analysis and device control that prompts the solar PV panel to maximize overall performance [11].

Multmer and Erat A designed an intelligent cleaning system using fuzzy logic to clean the panels automatically. It was made with Arduino as the microcontroller. The cleaning system uses membership functions of the fuzzy logic like panel temperature, shadowing, dusting and output current that enables its efficient operation. Two membership functions were calculated for each of those input functions. Specific detail on the membership functions of system inputs is described in the section on system architecture. Those membership rolls determine whether or not to activate the program. The design goal is to eliminate efficiency losses due to dusting and dirt on the surface of the panel and to allow maximum generation of electric energy. As a result, the lack of energy input is reduced without waiting for the cleaning time and the output has been improved by 15-20 per cent [12].

Nasib Khadka et al. demonstrate a smart robotic system describes a prototype's architecture and production process along with its testing on a photovoltaic demonstration module; moreover, it portrays the Implementation of the model built for large-scale solar farms. This system's prototype includes a robot for cleaning and a cloud interface. The robot cleans the entire solar panel system by rotary cleaning brush through the back and forth motion of the rotary cleaning. The cleaning robot is mobile. Furthermore, a sensing device composed of sensors was connected to this network to inform the performance of distantly located solar farms, that updates the farm's input and output parameters to the cloud interface. In comparison, in this analysis, completely clean and dusty panel

data lasted for a month, regression analysis was conducted and the regression model was developed to determine the correct cleaning period. For a large-scale solar farm with a sensing device that detects the farm's conditions robotic device robots mounted on each series of solar farms that perform cleaning action if and only if, The order is sent from the operator or the sensing device; and the cloud interface interfacing the smart photovoltaic panel cleaning system for each and every device [13].

Gargi Ashtaputre and Amol Bhoi present an autonomous robot that cleans the panel smartly and at low cost is developed. The project is split into two parts: System Cleaning and System Monitoring. Cleaning function is performed according to control device data obtained. Wireless infrastructure was applied to capture all the data from a single stand. Panel's power output is tracked carefully, and the cleaning action is activated based on the information gathered at each node. This system detects panel breakage, too. The device has the ability to run remotely, so users from any part of the world are able to access all field knowledge [14].

Babu K et al. show the performance of the PV module is tested for different types of pollutants. The drop in voltage of the PV module and the output power depends on the mass accumulated and the type of pollutant. The methodology of cleaning and carrier robots is used where the carrier robot detects the edges of the solar panel with the help of IR sensors that are used to sense the start and end of the panels. The movement of the carrier robot is performed by the driver circuit [15].

## 1.2 Market survey

To understand the current market scenario of the cleaning robot for solar panels, a market survey was conducted by visiting the industries manufacturing and selling the robots. This study helped in making improvements in the model. The cleaning robots existing in the market are given below.

### 1.2.1 Aegeus Semi-automated robot

It is a semi automated cleaning robot that is waterless and utilizes a dry system of cleaning using soft microfibre brushes. The solar panel is mounted with a docking station in order to charge the robot for the cleaning operation. The robot will not start cleaning and will continue to stay at the docking station if there is not enough charge in the robot or it will return to the docking station if it is under operation.

### 1.2.2 Aegeus Unicorn

Aegeus Unicorn, as shown in Figure 1.2, is a self powered and self cleaning smart robot that can acquire weather information, sense dust levels on the panel and differentiate dust from bird droppings or panel breakage as it is an IOT/Cloud connected robot with features of machine learning. It acts according to the information acquired. For example if rain is predicted the robot does not operate.



Figure 1.2: Aegeus Unicorn

### 1.2.3 Aegeus Shreem

Aegeus Shreem shown in Figure 1.3 is a compact small-sized cleaning robot used for rooftop solar projects. It operates on Airwash technology and hence water or harmful chemicals are not used. The brushes of the robot are of soft microfibre cloth (Axial Radial). The controlled air flow mechanism enables the robot to clean the panels efficiently ensuring that all the dust is cleaned from the panel edges. This robot can approximately clean 200 panels in an hour and it can be carried easily from one location to the other.

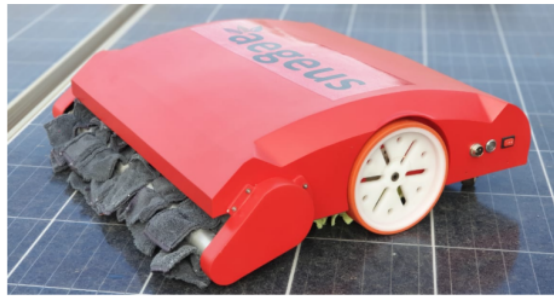


Figure 1.3: Aegeus Shreem

#### 1.2.4 Taypro 2.0 basic

It is a fast and effective waterless solar panel cleaning robot compatible with various tilt configurations of the panel. It is designed to work for both utility scale and rooftop solar plants that are not specifically designed for robotic cleaning with minor infrastructural modifications, shown in Figure 1.4.



Figure 1.4: Taypro 2.0 Basic

#### 1.2.5 Taypro 2.1 Automatic

Taypro 2.1 Automatic, as shown in Figure 1.5, is used on solar panels of different sizes. It can run on solar panels with irregularities between them. The robot provides scratch free cleaning of the panels automatically on the scheduled time along with giving weather updates and a long lasting battery life.



Figure 1.5: Taypro 2.1 Automatic

### 1.3 Motivation

As there is a need for the usage of renewable energy sources for power generation, solar energy is considered to be one of the important sources of electrical power generation.<sup>39</sup> Also, the world is becoming more conscious about solar power. Hence, there is a greater need to build effective solar power plants and proper maintenance systems for the plants to assure optimum power generation. Accumulation of dust on the solar panels decreases the power output in considerable amounts and the power loss is huge in large power installations. Cleaning the solar panels regularly ensures greater working efficiency as accumulation of pollutants affects the performance of solar panels. Need for developing a cost effective and IOT based model of cleaning robot applicable in different weather conditions, and also ensuring the effective cleaning in the presence of different kinds of pollutants is a major motivating factor to carry out this work.<sup>2</sup>

### 1.4 Problem Statement

“To design and fabricate a solar PV cleaning robot and conduct tests to analyze the performance of the solar panels.”

### 1.5 Objectives

The primary objective was defined as the implementation of an autonomous solar PV cleaning robot to increase their efficiency. The objectives were further defined through the following:

- To study the various models of cleaning systems available for solar panels.

- To design a control circuit for the movement of the cleaning robot along the panel and operation of cleaning brushes.
- To implement a prototype for the robot.
- To design and fabricate a solar PV cleaning robot.
- To perform various studies to check and analyze the performance of the robot on monocrystalline and polycrystalline solar panels.

## 1.6 Brief methodology

The development methodology for the project is shown in Figure 1.6. In the earlier stages of the project, a detailed literature study is carried out to understand the need for the development of a cleaning robot for the solar panels. Along with the literature survey, market survey is also conducted by visiting industries. Based on the literature studies and market survey the problem statement is defined. The problem statement is defined to reflect the innovative nature of the project by adding features that are not already present in the industry. Due to extensive market research, the key functionalities and design of the robot were changed that includes changing the powering and charging mechanism, design and material of brushes as well as incorporating key demands by the customer i.e, water cleaning. The robot has been ingeniously constructed with easy to find local components that are low in cost, hence affords easy replicability in remote areas.

The robot consists of two parts namely dry cleaning and wet cleaning. In the dry cleaning, the 10 inch nylon brushes rotate at high speeds to clean the surface of solar panels of any dust particles. Additionally, due to the high speed air produced, the dust is pushed out farther away from the brushes and panel. These brushes are powered by 12V 350RPM Johnson DC Geared motors. The second part is the wet cleaning. It involves a rectangular rush along the panel with water running through pipes cleaning the panel as the robot moves along. The water comes from an overhead tank connected with a capacity of 1 liter. The robot is supported by the four drive wheels and four support wheels. The drive wheels are powered by a heavy duty DC geared motor and they run along the rim of the solar panel. The support wheels are at an angle 90 degrees to the

drive wheels. These run along the outer edge to provide additional support for the robot such that it does not slip.

All the above-mentioned components are controlled with the help of Arduino UNO and host of other sensors including irradiance, dust, etc. The heavy duty DC geared motors are controlled with the help of a L298N motor driver. The robot is currently powered by two 12 V 7Ah batteries. Dust analysis is performed to analyze the effect of dust on the panel efficiency by plotting the IV and PV curves. Further the performance is analyzed based on the dry cleaning and wet cleaning effect of the robot on the panels and the efficiency is compared.

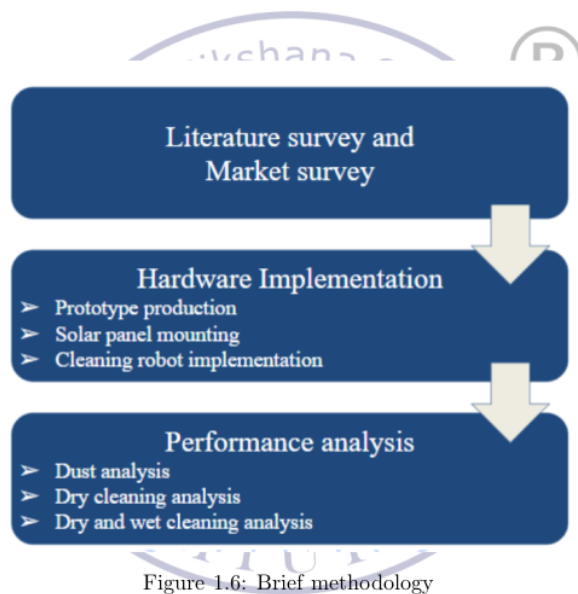


Figure 1.6: Brief methodology

## 1.7 <sup>34</sup> Organization of Report

This report is organized as follows:

- Chapter 1: Presents the brief introduction to the project and throws light on the topic in the form of literature review, motivation, problem statement, objectives and brief methodology of the project.
- Chapter 2: Briefs about solar energy, solar panels, factors affecting the performance of solar panels and various existing solar panel cleaning modules.

- Chapter 3: Highlights about the components used and the factors considered while selecting the components.
- Chapter 4: Discusses about the controlling methods incorporated in the robot.
- Chapter 5: Presents the results <sup>36</sup> of the robot.
- Chapter 6: Explains the conclusion and future scope of the project.



## CHAPTER 2

# FUNDAMENTALS AND PERFORMANCE ANALYSIS OF SOLAR PANELS

This chapter discusses briefly about types of PV modules, factors affecting the performance of PV modules and the various existing cleaning methods for solar panels [12]. The performance of solar panels is affected by a number of variables, including dust on the panel, temperature, weather conditions, soiling, degeneration of panels among others. Also, to ensure the better efficiency of solar panels, various cleaning systems are available in the market [16].

### 2.1 Solar Energy

The term “photovoltaic” is derived from two words, “photo” denoting light and “volt” denoting electrical energy. Therefore photovoltaic energy is the transformation of light <sup>58</sup> energy into electrical energy. Generally silicon <sup>62</sup> is employed as a photodiode to convert light energy into electrical energy [5]. If a PV cell is exposed to sunlight, it absorbs the hitting of the photons. As a result, electrons get excited and move to a higher orbit. To dissipate the extra amount of energy, an electron travels to the electrode thereby generating the potential. On an average a cell generates a potential up to 0.5 volts and cells are connected in series to get higher voltages [16]. Types of PV modules and performance analysis of solar panels under the influence of dust is discussed in following sections.

### 2.2 Solar Panel Modules

Several solar cells constitute together to form a solar module. Generally, a 250W module consists of 6X10 cells arranged in series and each module is rated from 100 to 360W. The specifications of the module are mentioned on the panel that includes power rating, open circuit voltage, short circuit current, current at peak power, voltage at peak power etc. The efficiency of the solar panels falls generally within 12 to 18% [8]. While

calculating the efficiency of solar panels a standard insolation of 1kW/sq. m is considered.

## 2.3 Types of PV Panels

Most of the solar panels used today are classified as <sup>21</sup> three types:

- Monocrystalline solar panels
- Polycrystalline solar panels
- Thin film solar panels

<sup>60</sup> Each type has its own advantages and limitations. Depending on the type of installation, cost consideration and usage suitable panels are chosen [6]. Each type of PV panel is discussed in the next subsections.

### 2.3.1 <sup>59</sup> Monocrystalline Solar Panels

Monocrystalline Solar Panels have cells made of silicon wafers. These types of panels differ from polycrystalline in composition of silicon itself. These <sup>13</sup> are made from a pure, single silicon crystal. Out of the three varieties, monocrystalline panels are the most efficient, with efficiencies exceeding 20%. These panels often have more than 300 W <sup>21</sup> and are more expensive than other types of panels [15]. The external appearance of monocrystalline panels is shown in Figure 2.1.

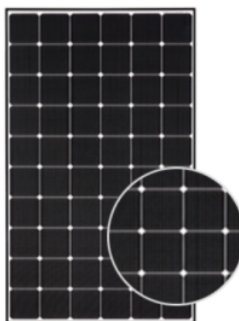


Figure 2.1: Monocrystalline Solar Panel

### 2.3.2 Polycrystalline Solar Panels

Despite having silicon-based cells, polycrystalline solar panels differ from monocrystalline panels. The external appearance of polycrystalline panels is shown in Figure 2.2. These panels' cells are made of Si crystal shards that have been fused together in a mold and then sliced into wafers. Cells of these types of panels are composed of fragments of Si crystals melted together in a mold before being cut into wafers. These types of panels have the efficiency range between 15%-17% and generally, they come as 250 W panels [11]. The cost of polycrystalline solar panels is less compared to monocrystalline panels.



Figure 2.2: Polycrystalline Solar Panel

### 2.3.3 Thin Film Solar Panels

Thin film solar panels are made from a different type of material. The most common is cadmium telluride (CdTe) and it is placed between transparent conducting layers to capture sunlight. Amorphous silicon (a-Si), Copper Indium Gallium Selenide (CIGS) and other types of materials are also used. These solar panels efficiency is about 11% that is lower than the other two varieties. Thin film solar panels come in 60,72 and 96 cell variants and are portable, lightweight and flexible [1]. The external appearance of a thin film solar panel is shown in Figure 2.3.



Figure 2.3: Thin Film Solar Panel

## 2.4 Problems Faced in Solar Power Plants

It is known [55] that the efficiency of solar panels is very low. The presence of dust and other pollutants reduces the efficiency further. The dust on the panel, along with blocking the irradiating light on the panel, also reduces the area that receives solar energy and makes non uniformity in the radiation spread over the surface of the panel. Thus, reduces the overall power generation [2].

The factors affecting the performance of solar panels are explained as follows:

- Dust: The IV characteristics of panel with and without accumulation of dust on the panel is shown in Figure 2.4. The current reduces with the accumulation of the dust resulting in the reduction of the power output [17].

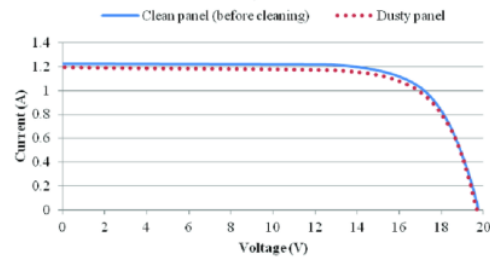


Figure 2.4: I-V Curve of Panel in Presence of Dust [18]

- Soiling: The accumulation [35] of snow, dirt, dust, leaves, pollen and bird droppings [46] on solar panels [46] is referred to as soiling. A PV module's performance decreases by [9] surface soiling and the PV power loss increases as the amount of soil on the module increases. Thus, the accumulation of soil on the PV module leads to a significant

decrease in energy produced by the PV module. The condition becomes even worse in some situations such as snowfall on PV modules because snow completely covers the surface of the PV module and no energy is produced at all.

- Radiations and atmosphere: The power output also depends on irradiation and atmosphere. The influence of weather and time on solar output is shown in Figure 2.5.

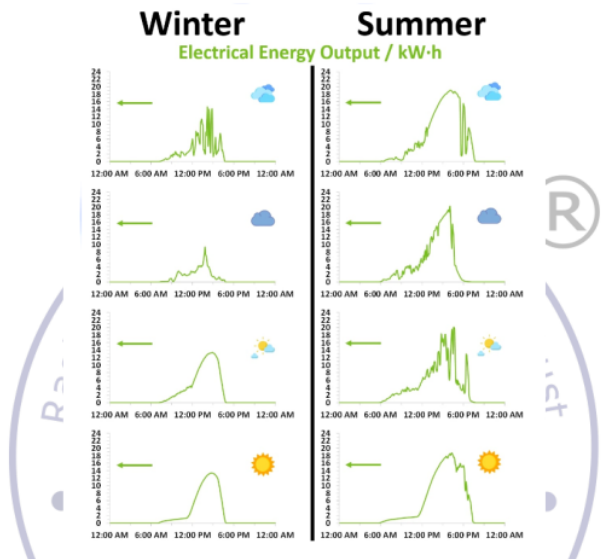


Figure 2.5: Solar Output in Different Weather and Time [18]

- Moisture and dew: Humidity drastically affects the performance of the Solar Panel and proves out to decrease the power produced from the Solar Panels up to 15-30% if subjected to an environment of high humidity.
- Temperature: Temperature plays another major factor in determining solar cell efficiency. As the temperature increases the rate of photon generation increases thus reverse saturation current increases rapidly and this reduces the band gap. Hence this leads to marginal changes in current but major changes in voltage. The cell voltage reduces by about 2.1mV per degree rise in temperature.
- Wind speed and direction: With the increase in wind speed, surface temperature on the solar panel reduces. Thus, results in an increase of efficiency to greater extent.

- Degeneration of panels: Over a period of time, solar cells may be subjected to some non-recoverable damages due to cracking, oxidation, irreversible soiling as shown in Figure 2.6. They cause reduction in short circuit current and increase in cell temperature that in turn affects the performance of the panels [17].

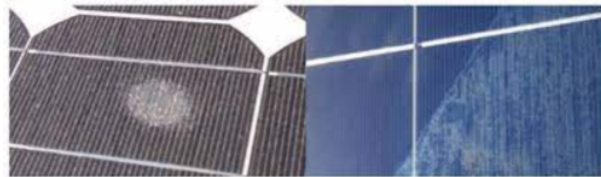


Figure 2.6: Degenerated Cell

## 2.5 Dust Accumulation and its Effects on Performance of Solar Panels

### 2.5.1 Causes of Dust Accumulation

There are a lot of factors that affect the accumulation of dust on the solar panel. It could vary from the location, altitude, latitude, climatic factors and so on. The various causes of dust accumulation are shown in Figure 2.7.

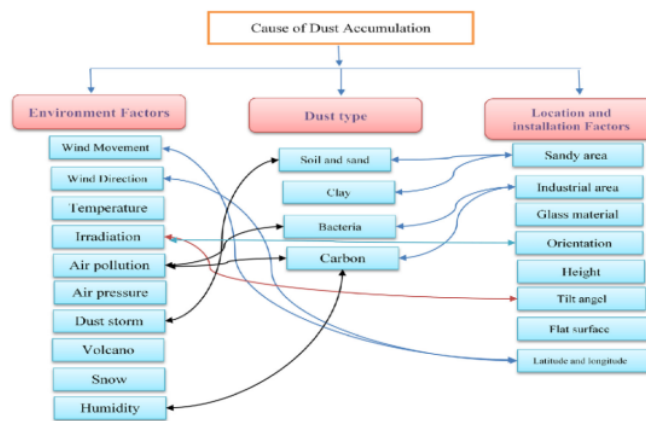


Figure 2.7: Causes of dust accumulation

- Environmental factors

These are the factors that are controlled by nature and it is tough for humans to predict, intervene and stop the soiling process. It also depends on the climatic and periodic weather conditions of the place. Some of the factors include wind movement,<sup>47</sup> wind direction, temperature, irradiation, air pollution, air pressure, dust storm, volcano, snow and humidity. Certain conditions like snow and volcanoes occur in few regions and are non significant factors in the soiling process. The most important ones in urban scenarios are air pollution, temperature, humidity and wind direction speed.

- Location and installation factors

Dust accumulation also depends on the location, installation of the panels and the spread of dust on the panels. If the panels are flat and are rested on a high surface, then the chances that the dust is uniformly spread are high. If the panels are inclined in a particular direction then the dust accumulation will be more towards the edges. If wind is not flowing then soiling occurs away from the corners. The glass material also matters at times. If the panels are located near industrial areas and regions of high vehicular movement, soiling is severe. Latitudes and longitudes are also considerable factors as they influence the weather factors and local climatic regions. Apart from these factors, the maintenance of the panels is also very important. If the panels are well maintained, then soiling will be slower otherwise, it erodes the glass surface and soiling will be accelerated.

### 2.5.2 Effects of Dust Accumulation

There are a lot of effects caused by soiling of solar panels that affect the functioning of a solar panel. The prominent ones are:

- Reduction in performance of solar panels.
- Damage on the outer surface of the solar panel.

### 2.5.3 Solar panel characteristics

The general solar panel characteristics that determine its performance are:

- <sup>38</sup> Short circuit current ( $I_{sc}$ ) - The maximum current that flows through a solar cell as the output terminals are shorted together.
- <sup>25</sup> Open circuit voltage ( $V_{oc}$ ) - The maximum voltage that the solar panel provides as the output terminals are not connected to any load.
- Irradiance ( $I$ ) - It is the measure of solar power and is defined as the rate the solar energy falls on a surface area ( $A$ ). Its unit is  $\text{kW/m}^2$
- <sup>11</sup> Maximum power point (MPP) - It is the point on the IV curve of a solar panel that relates to the maximum power generated as connected to a load.
- <sup>6</sup> Fill factor (FF) - Fill factor is the ratio of maximum power from the solar cell to MPP. It determines the power conversion efficiency of a solar cell and hence its quality. Ideally  $FF=1$ . Practically its value ranges from 0.5-0.8
- Efficiency (%) - Efficiency is defined as the ratio of maximum solar power generated <sup>20</sup> to the amount of irradiance hitting the solar panel. The efficiency of a solar panel depends on the type of solar panel. For monocrystalline it is around 22%. For Polycrystalline it's 14% and for thin film it is around 12%.

Figure 2.8 shows the IV & PV curve of a solar panel.

## 2.6 Dust analysis on Solar Panels

The dust analysis has been conducted on both <sup>13</sup> monocrystalline and polycrystalline panels. <sup>54</sup> The specifications of both the panels are shown in Table 2.1.

Table 2.1: Specifications of Monocrystalline and Polycrystalline test panel

Parameter	Monocrystalline	Polycrystalline
Power rating	265 W	250 W
Open circuit voltage	46 V	37.1 V
Short circuit current	7.59 A	8.6 A
Voltage at maximum power	39 V	30.5 V

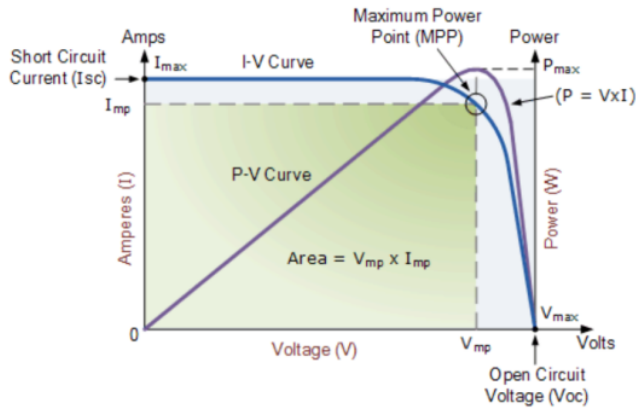


Figure 2.8: IV &amp; PV curve of solar panel [17]

Both the solar panels set up has been installed on the terrace in the EEE department, RVCE. They are inclined to about 18 degrees facing south to allow maximum sunlight to fall on the panels considering the latitude, longitude and the time of the year. The setup is also vulnerable to rainfall. The experiment is conducted in the month of July at around noon. The average temperature was 23 degrees in July. The experiment setup is shown in Figure 2.9 and 2.10.



Figure 2.9: Experiment setup for polycrystalline panel

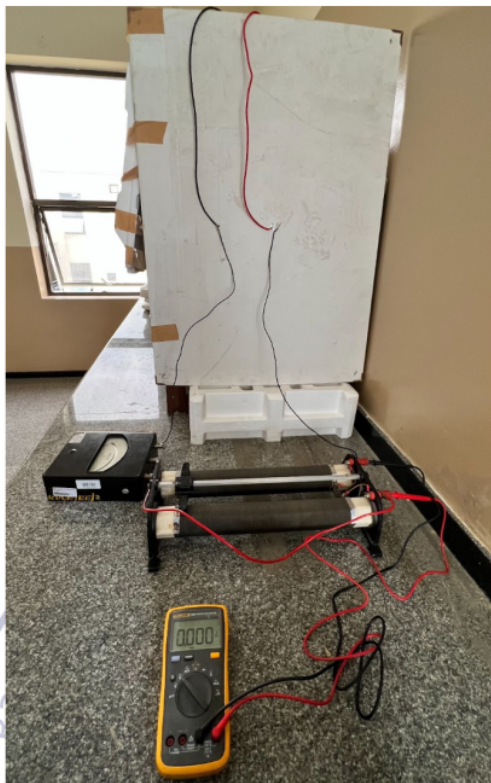


Figure 2.10: Experiment setup for monocrystalline panel

The values of current and voltage are calculated by varying the rheostat and eventually brought to cut in position. With the values of current and voltage, the values of power, fill factor, MPP and thus the efficiency are found. The graph of current v/s voltage (IV) and power v/s voltage (PV) is plotted. From the IV-PV graph, it is seen that the current remains constant and the value of current when the voltage is zero is called Short circuit current and after a certain voltage, the value of current starts to decrease and the power starts to increase and at a particular point, it attains maximum value. This point is called the Maximum Power Point of a solar cell. Beyond this point, both the current and voltage start to decrease drastically to a voltage known as Open circuit voltage.

Natural soiling on both polycrystalline and monocrystalline solar panels is as shown in Figure 2.11.



Figure 2.11: Natural soiling on polycrystalline and monocrystalline panel

Artificial soiling was done to analyze the performance of solar panels before and after the dry cleaning action of the robot. The artificial soiling on the polycrystalline and monocrystalline solar panels is displayed in Figure 2.12 and 2.13 respectively.



Figure 2.12: Artificial soiling on polycrystalline panel



Figure 2.13: Artificial soiling on monocrystalline panel

Monocrystalline and polycrystalline solar panels after being cleaned with the robot are displayed in figure 2.14.



Figure 2.14: Solar panels after dry cleaning

## Summary

The basics of solar technology, types of solar panel modules and the factors affecting the performance of solar panels were discussed. A detailed explanation of dust analysis and the setup was presented.



## CHAPTER 3

# DESIGN AND DEVELOPMENT OF CLEANING ROBOT

While developing the customized model of robot, various parameters have to be considered including type of material for actuation system, motors for the brushes, motors for the movement of robot, types of brushes, controlling mechanism, types of sensors etc. The current chapter deals with the selection criteria and design of specifications of these components [4].

### 3.1 Selection of Drive Principle

Solar panels are not built to carry the weight of the robot. Drive principle is required to move the robot on the sides of the panel with the help of rails. The selection of drive principle is based on mechanical stability, effectiveness in cleaning and ease in building. Two types of drive selection are possible [17]. Both the principles are explained in the following subsections.

#### 3.1.1 Horizontal Rails with Vertical Brushes

The brush is vertically aligned to the direction of alignment of rails and moves horizontally with the help of the rail system as shown in Figure 3.1. If the dust on a slightly tilted solar panel is swept by the robot, it directly falls to the ground [17].



Figure 3.1: Horizontal Rails with Vertical Brushes

This kind of arrangement has certain advantages and disadvantages listed as follows:

Advantages:

- Clean many solar panels if connected through rails.
- Cleaning is more effective as there is no gap left.
- It is applicable to large solar installations.

Limitations:

- Cleaning takes a longer time.

### 3.1.2 Horizontal Rails with Horizontal Brushes

The arrangement with horizontal brushes has a complicated construction mechanism.

It is shown in Figure 3.2.



Figure 3.2: Horizontal Rails with Horizontal Brushes

The advantages and limitations of this kind of arrangement are listed as:

Advantages:

- Smaller brush is sufficient.
- Cleaning takes a shorter time.
- Applicable for residential panels as only one panel is normally sufficient.

Limitations:

- Clean only one panel at a time as there is no scope for continuous motion along the rows of panels.

Based on the comparison, the model with vertical brushes is found to be more applicable for large installations like power plants. If all the panels are connected with the rails, it is possible to clean all the panels that are connected [8]. The working mechanism of the robot model is explained in the next section.

### 3.2 Working Mechanism

The robot functions according to following mechanism:

- As soon as the start button is pressed, the system starts to function.
- Two control circuits are present: one for the movement of the robot and the other for the brushes. Both the circuits are responsible for the movements of corresponding motors respectively.
- The wet brush is provided behind the circular brushes to carry out the cleaning more effectively. It wipes off the left-out dirt with minimal water.
- As soon as the robot reaches the end, the limit switches send the signal to the controlling circuit to stop the movement of the brushes and robot and bring the robot to the original position.

### 3.3 3D Model of Robot

A 3D model of the robot has been developed using SolidWorks mechanical design software. The 3D model with three rotating brushes and one rectangular brush is shown in Figure 3.3 to 3.6. The proposed model consists of a horizontally moving robotic system with vertical brushes. The robot consists of three rotating brushes and one wet brush behind the rotating brushes. If any amount of dirt and dust are still left over, it is removed by the wet brush. The whole system is powered through the solar charged battery in the docking station. The controlling system is embedded in the robot with proper protection schemes. The robot is able to move along the panels with the help of wheels that are connected to the shaft of motor.

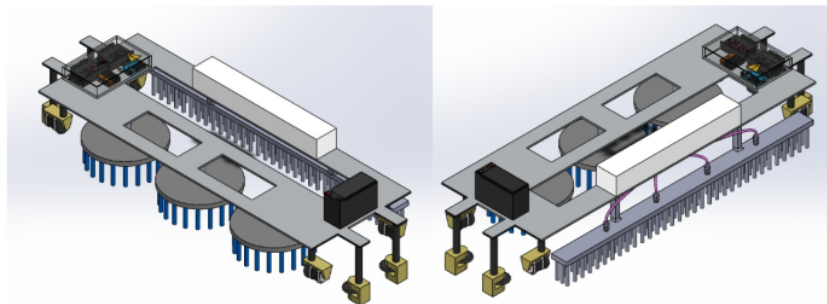


Figure 3.3: Isometric view of the robot

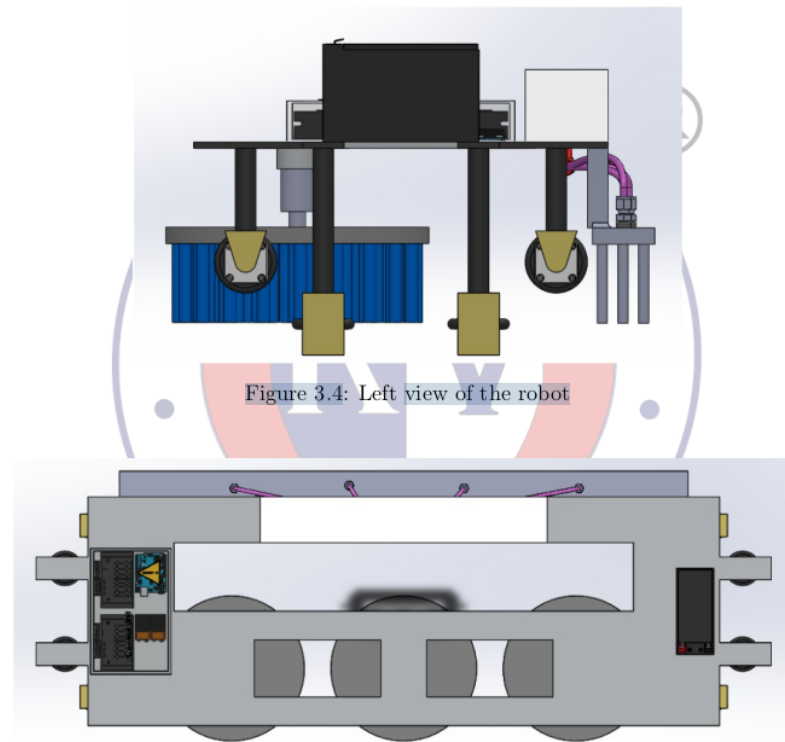


Figure 3.4: Left view of the robot

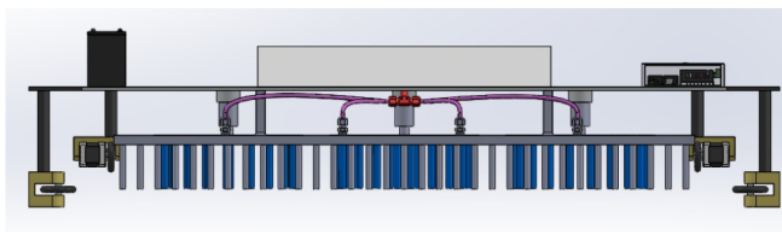


Figure 3.5: Top view of the robot



Figure 3.6: Side view of the robot

### 3.4 Specifications of Reference Solar Panel

The robot is designed for the reference panel of a 1.06kW system mounted at the EEE Dept. Of RVCE. It consists of two 265 W polycrystalline panels and two 265 W monocrystalline panels arranged in series as shown in Figure 3.7 and 3.8. The specifications of each panel are as shown in Table 3.1 and 3.2.



Figure 3.7: Solar panel installation

Table 3.1: Specifications of each Polycrystalline test panel

Parameter	Value
Power rating	265 W
Open circuit voltage	22.3 V
Short circuit current	15.1 A
Voltage at maximum power	18.5 V
Current at maximum power	14.2 A
Module efficiency	16.2%
No.of cells	64
Dimension	1645 mm x 990 mm x 35 mm

Table 3.2: Specifications of each Monocrystalline test panel

Parameter	Value
Power rating	265 W
Open circuit voltage	46 V
Short circuit current	7.59 A
Voltage at maximum power	39 V
Current at maximum power	7.16 A
Module efficiency	19.7%
No.of cells	72
Dimension	1355 mm x 990 mm x 35 mm

### 3.5 Linear Actuation System

Linear actuation system helps in movement of the robot along the panel. Wheels are attached to the shaft of the motor and the motor drives the wheels. Heavy duty DC geared motors are used for the movement of the robot through the rails.

#### 3.5.1 Design of Heavy duty DC geared motor

Ratings of the heavy duty DC geared motors are designed for the required torque and power ratings. Here, the radius of the shaft of the wheel is considered as 1.1 cm. Torque and power are calculated using equations (3.1) and (3.2) respectively. Motor for linear actuation is as shown in Figure 3.9.

- Radius of the shaft = 1.1 cm

- Torque,

$$T = F * r \quad (3.1)$$

- Power,

$$\text{Power} = (2\pi NT)/60 \quad (3.2)$$

The specification of the heavy duty DC geared motor is:

- V = 12 V
- N = 30 rpm
- P = 10 W
- T = 3.2361 N-m

#### 3.5.2 Specifications of Heavy duty DC geared motor

The specifications of each heavy duty Dc geared motor is given <sup>23</sup> in Table 3.3.



Figure 3.8: Heavy duty DC geared motor

Table 3.3: Specifications of heavy duty DC geared motor

Parameter	Value
Operating voltage	12 V
No load current	220 mA
Load current	1300 mA
No load speed	60 rpm
Rated torque	10 kg-cm
Shaft diameter	8 mm
Motor dimensions	70 x 70 x 90 mm

### 3.6 Driving Mechanism for Dry Cleaning Brush

The circular brushes employed for dry cleaning of the solar panels are powered by DC gear motors. A DC gear motor is an electrical device that transforms electrical energy supplied to mechanical energy by rotating the shaft attached to it. The input to the motor is in the form of direct current. In this robot, Johnson DC geared motors have been used to rotate the circular brushes. It is a DC motor with a gear box attached to its shaft. It is a mechanically commutated, direct-current electric motor (DC). The motor's speed is decreased while its production of torque is increased when a gear head is added.



Figure 3.9: Johnson DC gear motor

### 3.6.1 Design of DC gear motors

Ratings of the DC gear motors are designed for the required torque and power ratings. Here, the radius of the shaft of the brush is considered as 12.7 cm. Torque and power are calculated using equations (3.1) and (3.2) respectively.

- Radius of the shaft = 12.7 cm

- Torque,

$$T = F * r \quad (3.3)$$

- Power,

$$Power = (2\pi NT)/60 \quad (3.4)$$

The specification of the DC gear motor is:

- V = 12 V
- N = 350 rpm
- P = 45 W
- T = 1.2454 N-m

### 3.6.2 Specifications of DC gear motors

The specifications of each Johnson 12V DC gear motor is given in Table 3.4.

<sup>27</sup>  
Table 3.4: Specifications of DC gear motor

Parameter	Value
Rated voltage	350 rpm
Operating voltage(Vdc)	6.8 V
Nominal voltage	12 V
Rated torque	2.2 kg-cm
Stall torque	9 kg-cm
No-load current	300 mA
Load current	900 mA
Shaft diameter	6 mm
Motor dimensions	100 x 40 x 40 mm

### 3.7 Design of Docking Station

A docking station has been designed to charge the cleaning robot battery. This helps in reducing the overall weight of the robot as well as provide a docking space for the robot during unfavorable weather conditions. The docking station consists of a 100W auxiliary solar panel that is mounted on it, that will power the robot battery. The 3D model for the docking station is given in Figure 3.11.

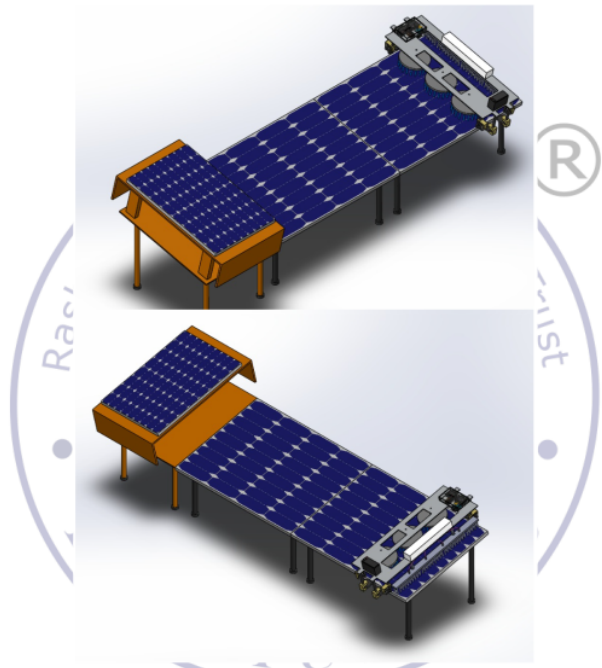


Figure 3.10: Isometric view of Docking station

#### 3.7.1 Auxiliary Solar Panel

Auxiliary solar panel of 100W is used to power the battery. The figure and specifications of auxiliary solar panel shown in Figure 3.12 and Table 3.5 respectively.

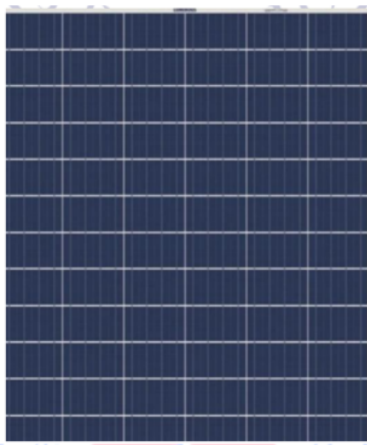


Figure 3.11: 100W Auxiliary Solar Panel to Power Battery

Table 3.5: Specifications of Auxiliary panel

Parameter	Value
16 Power rating	100 W
Open circuit voltage	22.05 V
Short circuit current	5.95 A
Voltage at maximum power	18.15 V
Current at maximum power	5.66 A
Module efficiency	14.58%
No. of cells	36
Motor dimensions	1010 mm x 665 mm x 34 mm

### 3.7.2 Battery Rating Calculations

The robot has 3 DC geared motors and 4 heavy duty DC geared motors for the operation of brushes and actuation systems. Solar battery that powers the motors is designed and required current capacity is calculated based on the motor ratings. The 12V system is considered for calculation purposes.

- Number of DC gear motors = 3 (each of 45W)
- Total power =  $3 \times 45 = 135$  W
- Number of heavy duty DC geared motors = 4 (each of 10W)
- Total power =  $4 \times 10 = 40$  W
- For 12 V system, current rating of battery =  $(135+40)/12 = 14.58$  A

- As the system runs for around 20-30 minutes at a time, two 7Ah batteries are needed.

### 3.8 L298N Motor Driver 43

L298N is a high voltage, high current motor driver module that is used to control stepper motors and DC gear motors. It 8 consists of an L298 dual-channel H-Bridge motor driver IC and uses two types of techniques 32 in order to control the speed and direction of rotation of DC motors. They are PWM and H-Bridge. PWM technique is used to control the speed of the motor and H-bridge 50 is used to control the direction of rotation of the motor. Two DC motors or one stepper motor can also be controlled by L298N at the same time. Motors with voltage varying from 5-35 Volts can be interfaced with this driver giving the maximum current of 2 Amperes. The two main key components of the motor driver are the L298 motor driver IC and the 5V regulator. The pin diagram of the L298N motor driver is shown in Figure 3.13.

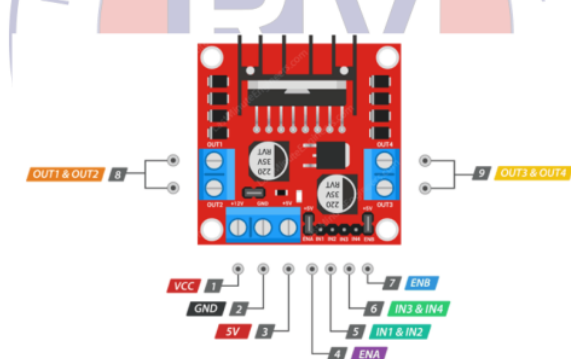


Figure 3.12: Pin Diagram of L298N Motor Driver

### 3.9 Arduino Uno

The microcontroller board that has been used for robot control is Arduino Uno 49 that 18 is based on the ATmega328. It has a total of 14 digital input/output pins. 6 pins are employed as PWM outputs, 6 pins as analog inputs, a 16 MHz ceramic resonator, an ICSP header, a USB connection, a power jack and a reset button as shown in Figure

3.14. Arduino is powered by a 12V battery and the code is uploaded by connecting it to a computer with a USB cable. The advantages of using Arduino Uno are:

- It can interface with USB easily.
- As it is an open source design it is very helpful in debugging projects as it has an advantage of usage by a large community of people.
- The serial communication assures easy protocol
- Has hardware features like timers, interrupts (both external and internal) PWM pins.
- Low cost

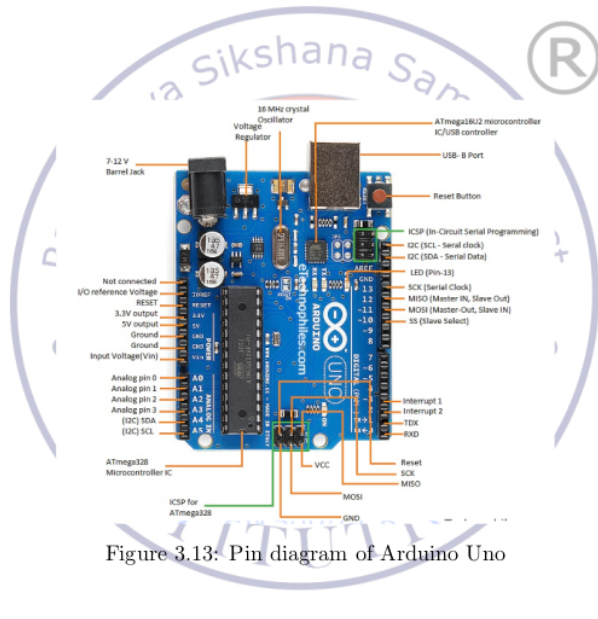


Figure 3.13: Pin diagram of Arduino Uno

### 3.10 Support Structure

The robot components are supported on an Aluminum frame made out of grade 6061 aluminum. Aluminum is chosen over other metals because of the following advantages -

- Light weight
- Corrosion resistant
- Recyclable

- Environment friendly
- Weather resistant

### 3.10.1 Properties of Aluminum 6061

Aluminum 6061 is an alloy majorly made up of silicon and magnesium by the process of precipitation hardening. It has medium to high strength and has good corrosion resistance, weldability, workability, and machinability. The summary of the general characteristics are as shown in Table 3.6.

<sup>10</sup>  
Table 3.6: Summary of mechanical properties of 6061 aluminum alloy

Mechanical Properties	Unit (Metric)	Unit (English)
Ultimate tensile strength	310 MPa	45000 psi
Tensile yield strength	276 MPa	40000 psi
Shear strength	207 MPa	30000 psi
Fatigue strength	96.5 MPa	14000 psi
Modulus of elasticity	68.9 GPa	10000 ksi
Shear modulus	26 GPa	3770 ksi
Electrical resistivity	$5.15 \times 10^{-6}$ ohm-cm	

Some of the applications of aluminum 6061 include -

- <sup>22</sup>Automotive industries
- Welded Assemblies
- Modern aircraft industries
- Building construction industry e.g. subway platforms, stairs, flooring, cover plates, walk away, and more.
- Electrical fittings.
- Chemical equipment

### 3.10.2 Frame Fabrication

The aluminum frame is cut by waterjet cutting, that is an engineering technique used to cut a huge variety of materials by a high pressure jet of water projected through a small precision nozzle.

### 3.10.3 Locomotion Unit

The robot is supported by the four drive wheels and four support wheels. The drive wheels are powered by heavy duty DC geared motors that run along the rim of the solar panel and support wheels, angled 90 degrees to the drive wheels, run along the outer edge of the panel to provide additional support for the robot so that it does not slip. The heavy duty DC geared motors are controlled with the help of L298N motor drivers that are controlled with the help of microcontroller Arduino UNO. The robot stops moving on the panel once the limit switch detects the end of the panel string.

## 3.11 Cleaning Brushes

The cleaning of the solar panels is carried out by the two different types of brushes, circular rotating brushes and rectangular brush. Cleaning is employed by two cleaning mechanisms namely dry cleaning and wet cleaning as explained in the following subsections.

### 3.11.1 Dry Cleaning System

The process of dry cleaning takes place with the help of three circular rotating brushes each of 10 inch diameter with 3 inch long nylon bristles. Each brush is attached with a 12V 350 rpm DC gear motor that is powered by a 12V, 7Ah battery resulting in their rotation. The dry brush attached with a DC gear motor is shown in Figure 3.15.



Figure 3.14: Brush for dry cleaning

### 3.11.2 Wet Cleaning System

Wet cleaning is carried out by a rectangular brush of length 37.4 inch and width 3 inch with 2 inch long nylon bristles. The brush comes with 8 water nozzles that are connected to the water storage tank to supply water through connectors and a valve. A sample figure is shown in Figure 3.16.



Figure 3.15: Sample image of brush for wet cleaning

## 3.12 Cost Estimation of Robot Model

Various components required to build the robot model are selected and designed based on requirements. Table 3.7 shows the estimation of the cost of the robot model.

Table 3.7: Cost Estimation of Robot Model

Component	Cost
Geared DC Motors (3 no's)	1100/-
Heavy duty DC geared motor (4 no's)	3800/-
Arduino Uno (2 no's)	2000/-
Motor driver - L298N (2 no's)	280/-
Cleaning brush - Circular(3 no's) + Rectangular (1 no.)	12350/-
Battery (12V 7 Ah) (2 no's)	1100/-
Solenoid valve	580/-
Robot fabrication	6500/-
Miscellaneous	5000/-
Total	32,710/-

## Summary

The drive principle was selected according to the requirements and the components were selected considering various properties and applications. The specifications of the components required for the robot were designed and specified for the proposed robot model and the cost of the model was estimated.



## CHAPTER 4

### DESIGN OF CONTROL CIRCUIT

The control circuit in a robot is responsible for monitoring the action of different components like sensors, motors etc. Proper functioning of a robot depends on the design and implementation of the control circuit [11]. The control circuit of the robot consists of motor control of geared DC motors. The present chapter discusses the controlling method used for geared DC motors.

#### 4.1 <sup>52</sup> Speed Control of DC Motor

The speed of DC motor is expressed by an equation

$$N = K(V - I_a R_a) / \phi \quad (4.1)$$

Where, V = Voltage applied

R<sub>a</sub> = Resistance of armature

I<sub>a</sub> = Armature current

$\phi$  = Flux

<sup>8</sup> From speed equation, speed of DC motor is:

- Inversely proportional to the flux produced by field windings,
- Directly proportional to the supply voltage.
- Decreases with increase in armature voltage drop.

Hence, the speed of a DC motor is controlled by,

- <sup>56</sup> Flux control method
- Armature voltage control method
- Supply voltage control method.

First two methods are not able to provide desirable speed control. Also, due to the flux control method there is a problem with commutation and armature voltage drop results in considerable power loss [14]. Hence, the supply voltage control method is often used. In supply voltage control method, most commonly used is the pulse width modulation technique discussed in the following subsection. It involves the generation of various pulses of different widths and its application to the motor driver. It is also advantageous because of the less power loss.

#### <sup>24</sup> 4.1.1 Pulse Width Modulation Method

In the Pulse Width Modulation method, the output signal is digital and is either zero(low) or one (high). Total time period is the sum of ON time and OFF time. In this technique Ton and Toff are varied to satisfy the required conditions. As Ton is increased, Toff decreases and vice versa. Output of Pulse Width Modulation pulses is as shown in Figure 4.1.

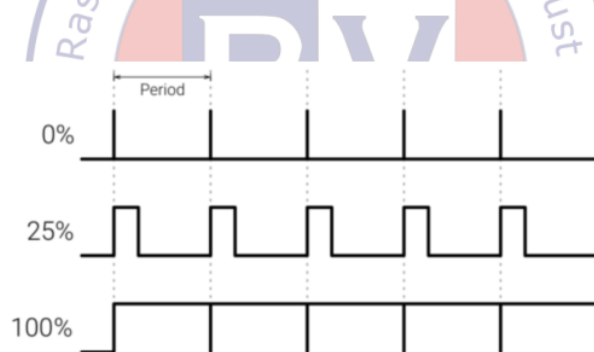


Figure 4.1: Output of PWM Pulses

Duty cycle is the fraction of one time period. Mathematically it is expressed as:

$$\text{Duty cycle} = (T_{on}/T) * 100\% \quad (4.2)$$

By varying the duty cycle, the speed of the motor is varied. If the duty cycle is zero, the motor doesn't start and if the duty cycle is one, the motor is expected to run at maximum speed.

#### 4.1.2 Direction Control of DC Motor

Direction control of DC motors is implemented with the help of H- Bridge shown in Figure 4.2. Direction of rotation is varied by closing particular switches. S1, S2, S3 and S4 are the logic switches and the direction of rotation of the motor depends on the control signal applied to the switches. The operation of the H-Bridge for various switching conditions is shown in Table 4.1.

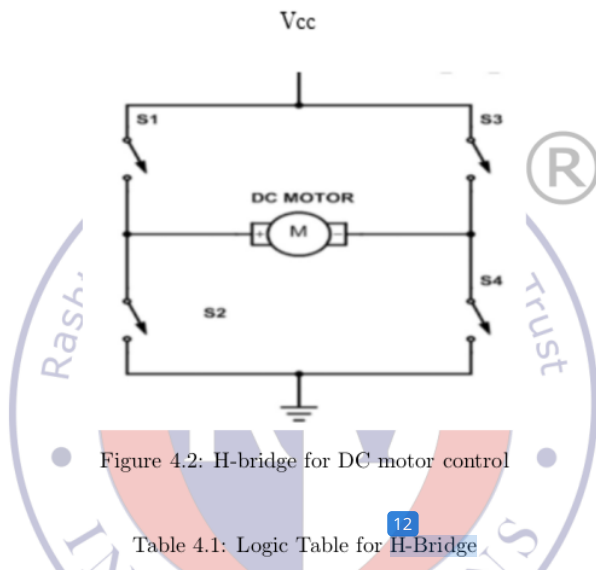


Table 4.1: Logic Table for H-Bridge

S1	S2	S3	S4	Result
1	0	0	1	Clockwise
0	1	1	0	Anticlockwise
0	0	0	0	Free run
0	1	0	1	Braking
1	0	1	0	Braking
1	1	0	0	Shoot through
0	0	1	1	Shoot through
1	1	1	1	Shoot through

Both direction and speed control are possible with the help of motor driver L298N. It is widely used for motion control of DC motors.

### 4.1.3 Interface of <sup>33</sup> heavy duty DC geared motors with L298N Arduino

To speed control the four heavy duty DC geared motors, two L298s are used. It has two output terminals to connect the motors in parallel and supplies a maximum current of 2A in each terminal. The board has 4 input pins and 2 enable pins for each motor. For motor A, the two input pins namely in1 and in2 are used to decide the direction of the motor whereas the enable pin is used to turn the motor ON or OFF. Additionally, it is also used to set the speed of the motor. Similarly for motor B identical connections are available.

<sup>11</sup> In order to control the speed of the motor, the enable pins are connected to the PWM pins of the Arduino. As the speed control in this project is done using the PWM (pulse width modulation) method hence the speed value is set between the values of 0-255, 0 corresponding to the motor being in OFF state and 255 corresponding to the highest RPM available by the motor that is 60 RPM in this case. The speed of the motors is set as 100 that roughly corresponds to 30 RPM. Figure 4.3 shows the circuit connection of the motors with L298N and Arduino Table 4.2 shows the pin connection.

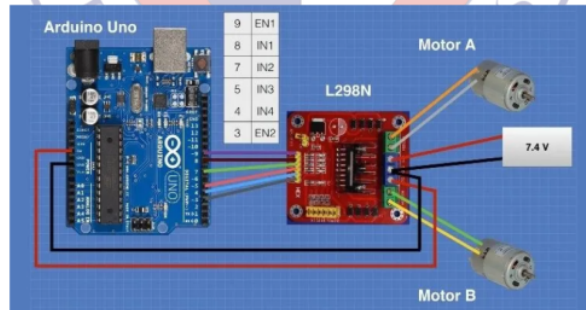


Figure 4.3: Interface of heavy duty DC geared motors with L298N Arduino

Table 4.2: Pin connections of L298N with Arduino

L298N pins	Arduino pins
enA	3
in1	2
in2	4
enB	5
in3	6
in4	7
enC	9
in5	8
in6	10
enD	11
in7	12
in8	13

## 4.2 Control of DC Motors for brushes

A small 12V relay is used to control the motors that are responsible for rotation of the nylon brushes. These relays simply act as ON and OFF switches for the motors so that the brushes can be controlled remotely. The three motors are connected in parallel to ensure same voltage across all the three motors leading to uniform speed of rotation of all the three brushes. The relay module has 3 input and 3 output pins. The input pins consist of 12V supply, IN i.e, input signal from Arduino and GND that is ground. The relay that has been used is shown in Figure 4.4.



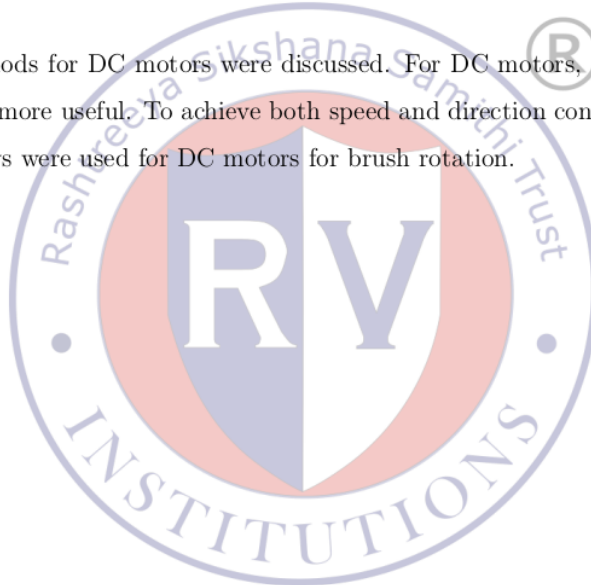
Figure 4.4: Relay used for cleaning brush control

The 12V pin is connected to the 12V DC battery, the IN is connected to pin number 1 of the Arduino and the GND is connected to the GND on the Arduino that is then connected to the negative terminal of the 12 DC battery. The output pins are NC, C, NO.

They stand for Normally Connected, Common and Normally Open respectively. Only two of the output pins are used according to the desired configuration required. For the purposes of this project normally open (NO) configuration is used where the common pin is connected to the 12V DC battery and normally open pin is connected to the one end of the motors. The motors are connected in parallel to the normally open pin. The other ends of the motor are connected to the negative terminal of the 12V DC battery. After making the connections a simple Arduino code (attached in the appendix) is used to control the rotation of the brushes of the robot.

## Summary

Control methods for DC motors were discussed. For DC motors, the PWM method was found to be more useful. To achieve both speed and direction control, motor drivers were used. Relays were used for DC motors for brush rotation.





## CHAPTER 5

### RESULTS & DISCUSSION

This chapter deals with the results and outputs obtained on various parts of the project namely dust analysis and the performance analysis of the cleaning robot. It also includes comparative study of dust analysis. The necessary graphs, images and tables are displayed to depict the results.

#### 5.1 Effect of dust on solar panels

Studies were conducted on both monocrystalline and polycrystalline solar panels to analyze the effect of dust accumulated on the panels on its efficiency. At STC (Standard Test Condition) that is temperature of 25°C and irradiance of 1kW, the efficiency of monocrystalline panel is 19.7% and polycrystalline panel is 16.2%. The average temperature while performing the experiment was 23.5°C.

##### 5.1.1 Polycrystalline panel

The analysis is performed on polycrystalline panel with a gap of 3 days and the corresponding voltage and current readings are noted.

**Day 1:** The readings for the polycrystalline panel on day 1 are as shown in Table 5.1 and Figure 5.1 shows the IV-PV curves of the readings obtained. The fill factor, MPP and efficiency are shown in Table 5.2.

Irradiance - 1,02,582 LUX / 810.39 W/m<sup>2</sup>

Temperature - 24°C

Table 5.1: Readings obtained for Polycrystalline panel - Day 1

Sl. No.	Voltage (V)	Current (I)	Power (P)
1	70.1	0	0
2	66.7	1.5	100.05
3	66.5	1.7	113.05
4	65.3	2.05	133.865
5	64.7	2.65	171.455
6	62.8	3.8	238.64
7	57.1	6	342.6
8	36.3	7	254.1
9	7.5	8	60
10	0	8.4	0

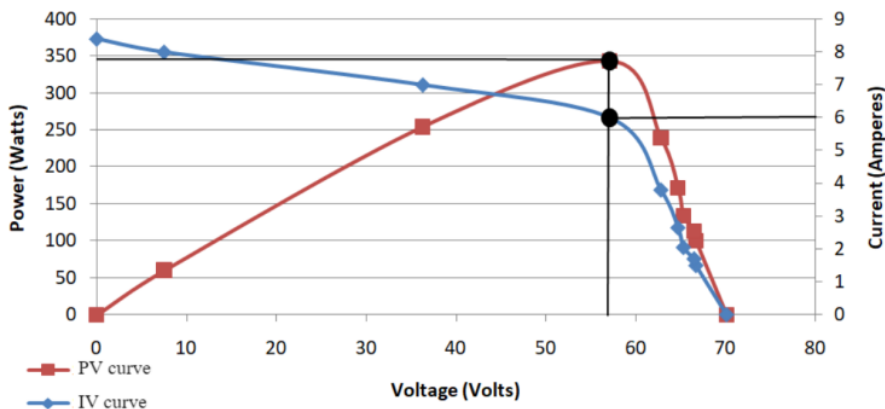


Figure 5.1: IV &amp; PV curve for polycrystalline panel - Day 1

Table 5.2: Parameters obtained for polycrystalline panel - Day 1

Sl. No	Parameter	Value
1	Short circuit current ( $I_{sc}$ )	8.4 A
2	Open circuit voltage ( $V_{oc}$ )	70.1 V
3	Fill factor (FF)	0.5818
4	Maximum power point (MPP)	342.6 W
5	Efficiency	12.98%

**Day 5:** The readings for the polycrystalline panel on day 5 are as shown in Table 5.3 and Figure 5.2 shows the IV-PV curves of the readings obtained. The fill factor, MPP and efficiency are shown in Table 5.4.

Irradiance - 1,01,049 LUX / 798.28 W/m<sup>2</sup>

Temperature - 23°C

Table 5.3: Readings obtained for polycrystalline panel - Day 5

Sl. No.	Voltage (V)	Current (I)	Power (P)
1	65.9	0	0
2	62.7	1.3	81.51
3	62.5	1.5	93.75
4	61.4	1.7	104.38
5	60.8	2.3	139.84
6	59	3.3	194.7
7	53.7	5.7	306.09
8	34.1	6.3	214.83
9	15.6	6.4	99.84
10	7.3	6.8	49.46
11	0	7.1	0

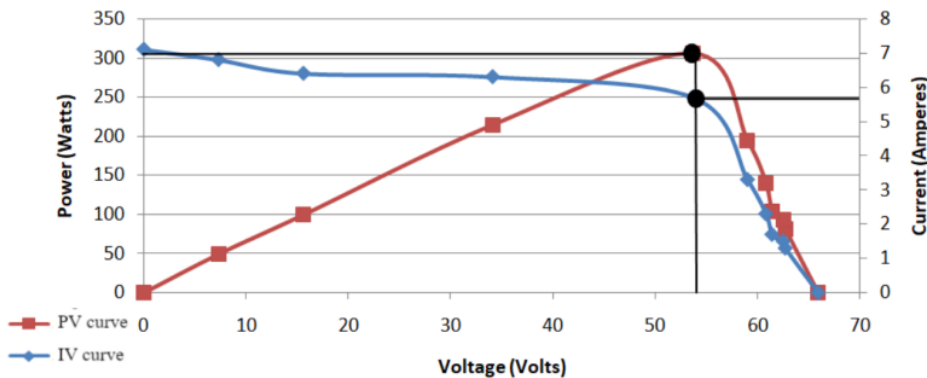


Figure 5.2: IV &amp; PV curve for polycrystalline panel - Day 5

Table 5.4: Parameters obtained for polycrystalline panel - Day 5

Sl. No	Parameter	Value
1	Short circuit current (Isc)	7.1 A
2	Open circuit voltage (Voc)	65.9 V
3	Fill factor (FF)	0.6541
4	Maximum power point (MPP)	306.09 W
5	Efficiency	11.77% percent

**Day 9:** The readings for the polycrystalline panel on day 9 are as shown in Table 5.5 and Figure 5.3 shows the IV-PV curves of the readings obtained. The fill factor, MPP and efficiency are shown in Table 5.6.

Irradiance - 102,049 LUX / 806.18 W/m<sup>2</sup>

Temperature - 23°C

Table 5.5: Readings obtained for polycrystalline panel - Day 9

Sl. No.	Voltage (V)	Current (I)	Power (P)
1	69.8	0	0
2	67.8	1.7	115.26
3	66.7	2.2	146.74
4	65.1	3.1	201.81
5	64.5	3.5	225.75
6	60.9	4.6	280.14
7	47.6	4.8	228.48
8	31.9	5	159.5
9	20.5	5.3	108.65
10	5.1	5.5	28.05
11	0	5.8	0

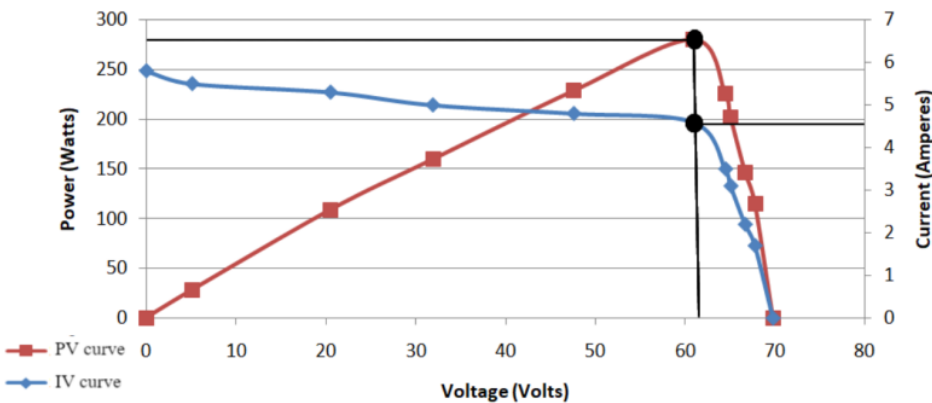


Figure 5.3: IV &amp; PV curve for polycrystalline panel - Day 9

Table 5.6: Parameters obtained for polycrystalline panel - Day 9

Sl. No.	Parameter	Value
1	Short circuit current (Isc)	5.8 A
2	Open circuit voltage (Voc)	69.8 V
3	Fill factor (FF)	0.6919
4	Maximum power point (MPP)	280.14 W
5	Efficiency	10.67%

### 5.1.2 Monocrystalline panel

The analysis is performed on monocrystalline panel with a gap of 3 days and the corresponding voltage and current readings are noted.

**Day 1:** The readings for the monocrystalline panel on day 1 are as shown in Table 5.7 and Figure 5.4 shows the IV-PV curves of the readings obtained. The fill factor, MPP and efficiency are shown in Table 5.8.

Irradiance - 1,02,582 LUX / 810.39 W/m<sup>2</sup>

Temperature - 24°C

Table 5.7: Readings obtained for monocrystalline panel - Day 1

Sl. No.	Voltage (V)	Current (I)	Power (P)
1	69.4	0	0
2	68.2	0.5	34.1
3	67.2	1.3	87.36
4	65.9	2.4	158.16
5	64.8	2.8	181.72
6	63	3.7	233.1
7	61.4	4.3	264.02
8	60.1	4.7	282.47
9	57.8	5.3	306.34
10	55.2	6	331.2
11	46.1	6.3	290.43
12	24.1	6.5	156.65
13	0	6.6	0

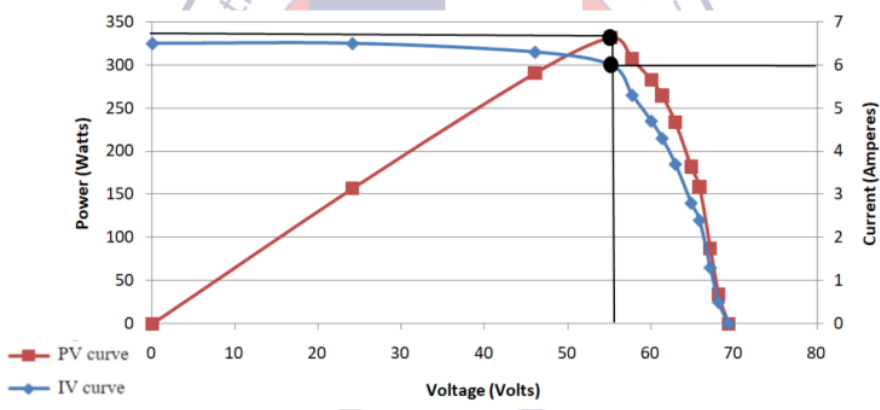


Figure 5.4: IV & PV curve for monocrystalline panel - Day 1

Table 5.8: Parameters obtained for monocrystalline panel - Day 1

Sl. No	Parameter	Value
1	Short circuit current (Isc)	6.6 A
2	Open circuit voltage (Voc)	69.4 V
3	Fill factor (FF)	0.7230
4	Maximum power point (MPP)	331.2 W
5	Efficiency	15.23%

**Day 5:** The readings for the monocrystalline panel on day 5 are as shown in Table 5.9 and Figure 5.5 shows the IV-PV curves of the readings obtained. The fill factor, MPP and efficiency are shown in Table 5.10.

Irradiance - 1,01,049 LUX / 798.28 W/m<sup>2</sup>

Temperature - 23°C

Table 5.9: Readings obtained for monocrystalline panel - Day 5

Sl. No.	Voltage (V)	Current (I)	Power (P)
1	64.8	0	0
2	63.9	0.4	25.56
3	63.3	0.6	37.98
4	62.1	1.3	80.73
5	60.3	2.6	156.78
6	58.8	3.4	199.92
7	57.9	3.9	225.81
8	54	5.3	286.2
9	52.5	5.4	283.5
10	47.1	6.4	301.44
11	44.4	6.5	288.6
12	30.6	6.7	205.02
13	12.3	6.8	83.64
14	0	6.8	0

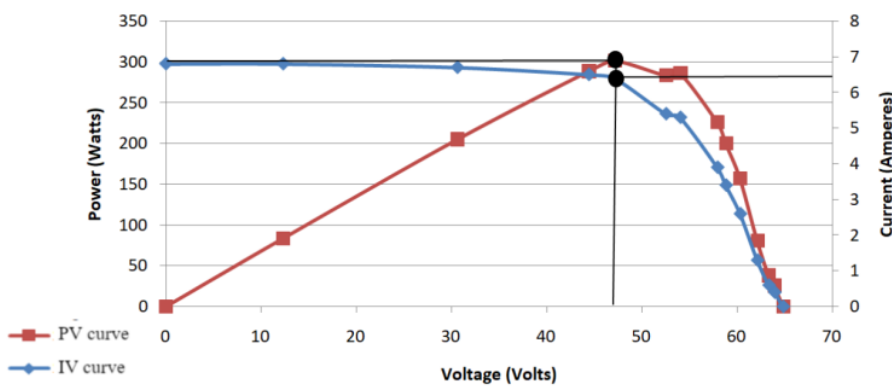


Figure 5.5: IV & PV curve for monocrystalline panel - Day 5

Table 5.10: Parameters obtained for monocrystalline panel - Day 5

Sl. No	Parameter	Value
1	Short circuit current (Isc)	6.8 A
2	Open circuit voltage (Voc)	64.8 V
3	Fill factor (FF)	0.6840
4	Maximum power point (MPP)	301.44 W
5	Efficiency	14.07%

**Day 9:** The readings for the monocrystalline panel on day 9 are as shown in Table 5.11 and Figure 5.6 shows the IV-PV curves of the readings obtained. The fill factor,

MPP and efficiency are shown in table 5.12.

Irradiance - 1,02,049 LUX / 806.18 W/m<sup>2</sup>

Temperature - 23°C

Table 5.11: Readings obtained for monocrystalline panel - Day 9

Sl. No.	Voltage (V)	Current (I)	Power (P)
1	84.8	0	0
2	82.6	2.4	198.24
3	79.6	2.9	230.84
4	77.2	3.3	254.76
5	74.7	3.7	276.39
6	63	4.1	258.3
7	49.1	5	220.95
8	35	4.9	171.5
9	24.2	5	121
10	13.1	5.1	66.81
11	7.1	5.4	9.18
12	0	5.5	0

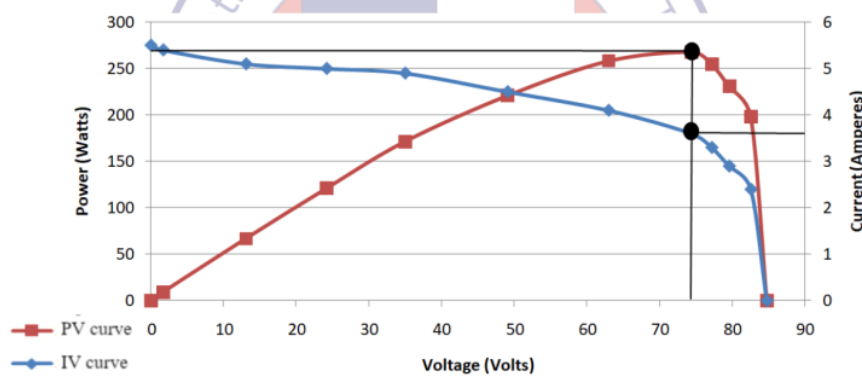


Figure 5.6: IV & PV curve for monocrystalline panel - Day 9

Table 5.12: Parameters obtained for monocrystalline panel - Day 9

Sl. No	Parameter	Value
1	Short circuit current (Isc)	5.5 A
2	Open circuit voltage (Voc)	84.8 V
3	Fill factor (FF)	0.5932
4	Maximum power point (MPP)	276.71 W
5	Efficiency	12.79%

### 5.1.3 Inference

- From Table 5.13, it is evident that as the days progress, there is a drop in the efficiency of the panels due to an increase in the dust accumulation on the panels.

This analysis is similar for both the types of panels.

- The efficiency of the panels is also affected by the weather conditions of that particular day.
- Monocrystalline panels get less affected by dust as compared to polycrystalline panels.

Table 5.13: Dust analysis results

Day	Temperature	Irradiance	Polycrystalline Panel efficiency(%)	Monocrystalline Panel efficiency(%)
Day 1	24°C	810.39 W/m <sup>2</sup>	12.98	15.23
Day 5	23°C	798.28 W/m <sup>2</sup>	11.7	14.07
Day 9	23°C	806.18 W/m <sup>2</sup>	10.67	12.79

## 5.2 Hardware implementation of the robot

The hardware model of the robot is as shown in the Figure 5.7, 5.8 and 5.9.

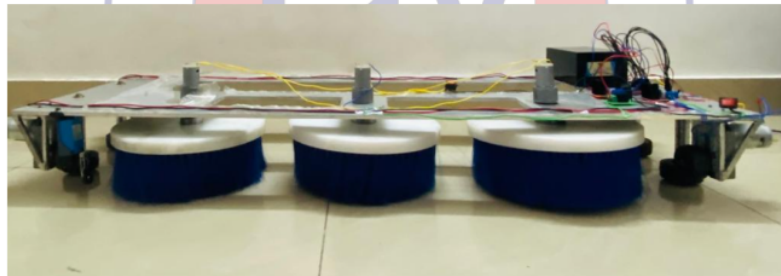


Figure 5.7: Robot model - side view



Figure 5.8: Robot model - top view



Figure 5.9: Robot on solar panel

### 5.3 Performance analysis of the robot

The performance of the robot is analyzed by comparing the efficiency of the panels after they are cleaned with the robot. The panels are subjected to artificial soiling with red sand of approximately 50 grams of dust and is spread evenly on monocrystalline and polycrystalline panels. The IV and PV curve is plotted for both the panels and the efficiency is calculated for panels with dust. The panels are then cleaned with the robot and again, the efficiency is calculated for clean panels. The efficiencies obtained in both the cases are compared to analyze the performance of the robot.

#### 5.3.1 Analysis after artificial soiling:

a) Polycrystalline panel: The readings noted for the polycrystalline panel after artificial soiling with red sand are shown in Table 5.14 and Figure 5.10 shows the IV-PV curves of the readings obtained. The fill factor, MPP and efficiency are shown in Table 5.15.

Irradiance - 1,01,887 LUX/ 804.90 W/m<sup>2</sup>

Temperature - 24°C

Table 5.14: Readings obtained for polycrystalline panel after artificial soiling

Sl. No.	Voltage (V)	Current (I)	Power (P)
1	64.7	0	0
2	64.1	3.1	198.71
3	63.8	3.1	197.78
4	63.2	3.6	227.52
5	62.1	4	248.4
6	60.2	4.5	270.9
7	57.7	4.9	282.73
8	48.5	5.2	252.2
9	38.3	5.8	222.14
10	28.1	6	168.6
11	19.9	6	119.4
12	9.2	6.5	59.8
13	4.7	6.7	31.49
14	1.5	6.9	10.35
15	0	7	0

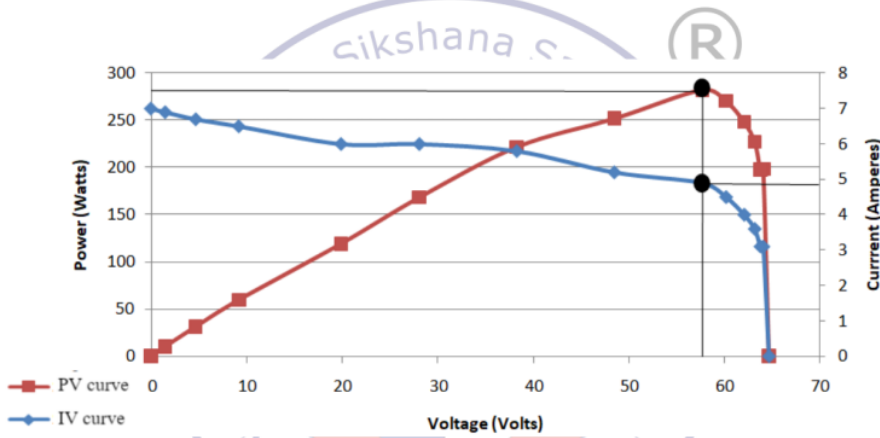


Figure 5.10: IV &amp; PV curve for polycrystalline panel after artificial soiling

Table 5.15: Parameters obtained for polycrystalline panel after artificial soiling

Sl. No	Parameter	Value
1	Short circuit current ( $I_{sc}$ )	7 A
2	Open circuit voltage ( $V_{oc}$ )	64.7 V
3	Fill factor (FF)	0.6242
4	Maximum power point (MPP)	282.73 W
5	Efficiency	10.78%

### b) Monocrystalline panel:

The readings noted for the monocrystalline panel after artificial soiling by red sand is shown in Table 5.16 and Figure 5.11 shows the IV-PV curves of the readings obtained.

The fill factor, MPP and efficiency are shown in Table 5.17.

Irradiance - 1,01,887 LUX/ 804.90 W/m<sup>2</sup>

Temperature - 24°C

Table 5.16: Readings obtained for monocrystalline panel after artificial soiling

Sl. No.	Voltage (V)	Current (I)	Power (P)
1	60.6	0	0
2	60.3	0.3	198.71
3	59.7	0.6	197.71
4	58.9	1.2	227.52
5	56.6	2.8	248.4
6	54.9	3.9	270.9
7	53.2	4.6	282.73
8	52.4	4.8	252.2
9	40.2	5	222.14
10	28.9	5.3	168.6
11	24.3	5.4	119.4
12	20.9	5.4	59.8
13	19.5	5.4	31.49
14	0	5.4	0

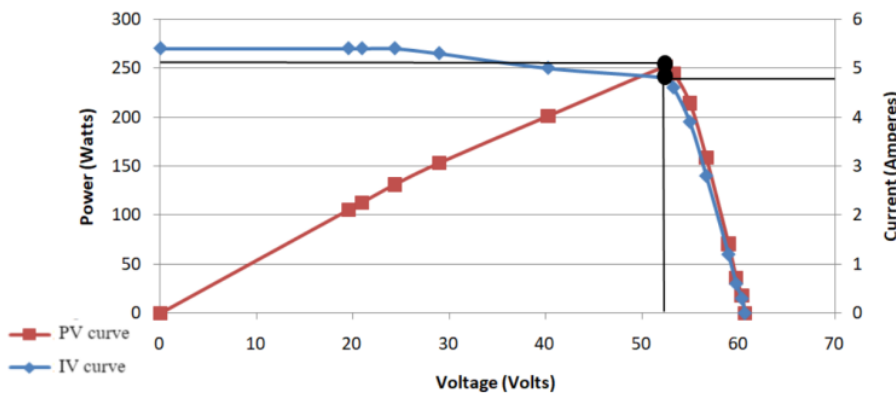


Figure 5.11: IV & PV curve for monocrystalline panel after artificial soiling

Table 5.17: Parameters obtained for monocrystalline panel after artificial soiling

Sl. No	Parameter	Value
1	Short circuit current (Isc)	5.4 A
2	Open circuit voltage (Voc)	60.6 V
3	Fill factor (FF)	0.7686
4	Maximum power point (MPP)	251.52 W
5	Efficiency	11.65%

### 5.3.2 Analysis after dry cleaning with the robot:

a) Polycrystalline panel:

4

The readings noted for the polycrystalline panel after dry cleaning is shown in Table 5.18 and Figure 5.12 shows the IV-PV curves of the readings obtained. The fill factor, MPP and efficiency are shown in Table 5.19.

Irradiance - 1,01,887 LUX / 804.9 W/m<sup>2</sup>

Temperature - 24°C

Table 5.18: Readings obtained for polycrystalline panel after dry cleaning

Sl. No.	Voltage (V)	Current (I)	Power (P)
1	70.1	0	0
2	67.2	1.8	120.96
3	66.4	2	132.8
4	65.7	2.3	151.11
5	65	2.6	168
6	64.69	3.1	200.26
7	63.2	3.6	227.52
8	61.4	4.4	270.16
9	57.7	5.2	297.28
10	45	6.2	297
11	23.3	6.2	144.46
12	14.5	6.5	94.25
13	3.6	6.5	23.4
14	0	6.8	0

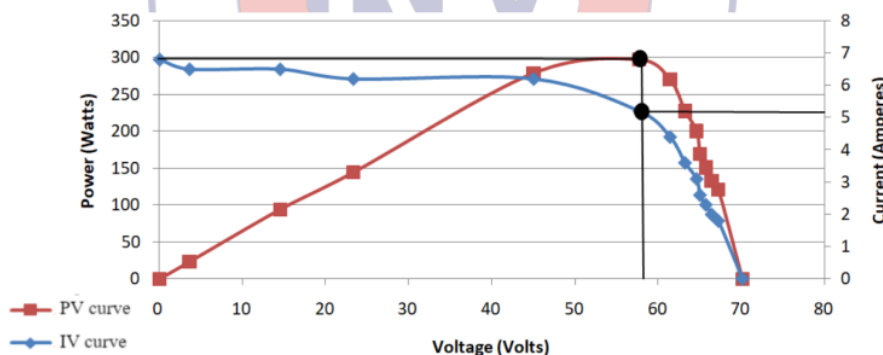


Figure 5.12: IV & PV curve for polycrystalline panel after dry cleaning

Table 5.19: Parameters obtained for polycrystalline panel after dry cleaning

Sl. No	Parameter	Value
1	Short circuit current (Isc)	6.8 A
2	Open circuit voltage (Voc)	70.1 V
3	Fill factor (FF)	0.6236
4	Maximum power point (MPP)	297.28 W
5	Efficiency	11.34%

b) Monocrystalline panel:

The readings noted for the monocrystalline panel after dry cleaning is shown in Table 5.20 and Figure 5.13 shows the IV-PV curves of the readings obtained. The fill factor, MPP and efficiency are shown in Table 5.21.

Irradiance - 1,01,887 LUX / 804.9 W/m<sup>2</sup>

Temperature - 24°C

Table 5.20: Readings obtained for monocrystalline panel after dry cleaning

Sl. No.	Voltage (V)	Current (I)	Power (P)
1	68.7	0	0
2	67.6	0.4	120.96
3	66.9	1.2	132.8
4	65.3	2.4	151.11
5	64.6	2.8	168
6	64.1.9	3.2	200.26
7	62.4	3.6	227.52
8	57.6	4.8	270.16
9	51.1	5.6	297.28
10	30	6.4	297
11	19.2	6.8	144.46
12	13.9	7.1	94.25
13	7.5	7.1	23.4
14	2.9	7.2	0
15	0	7.3	0

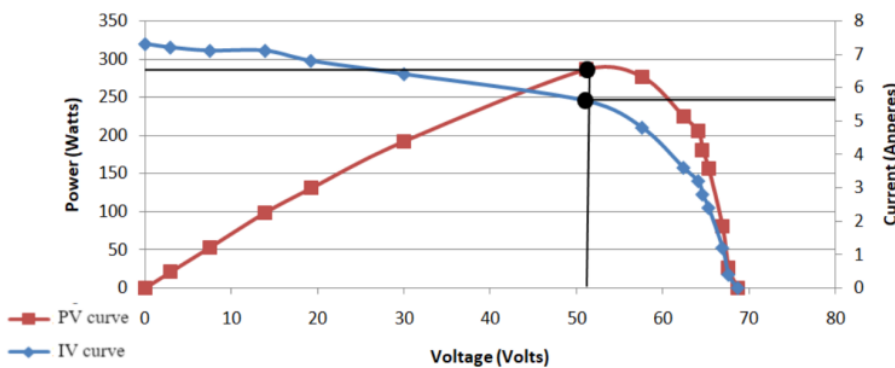


Figure 5.13: IV & PV curve for monocrystalline panel after dry cleaning

Table 5.21: Parameters obtained for monocrystalline panel after dry cleaning

Sl. No.	Parameter	Value
1	Short circuit current (Isc)	7.3 A
2	Open circuit voltage (Voc)	68.7 V
3	Fill factor (FF)	0.5705
4	Maximum power point (MPP)	286.16 W
5	Efficiency	13.24%

### 5.3.3 Inference

From Table 5.22 it can be analyzed that the efficiency of both monocrystalline and polycrystalline panels is improved after cleaning the panels with the robot.

- The efficiency of monocrystalline panels has increased from 11.34% to 13.24%.
- The efficiency of polycrystalline panels has increased from 10.78% to 11.65%.

Table 5.22: Performance analysis of the robot for dry cleaning

Type	Polycrystalline panels	Monocrystalline panels
Efficiency & MPP after artificial soiling with red sand	10.78%, 282.73 W	11.65%, 251.52 W
Efficiency & MPP after dry cleaning with robot	11.34%, 297.28 W	13.24%, 286.16 W

## Summary

In this chapter, the detailed results of the dust analysis for effect of dust on the panel efficiency and performance analysis were presented and the inference was discussed along with the hardware model of the robot with dry and wet cleaning.

## CHAPTER 6

### CONCLUSION & FUTURE SCOPE

As the world is more conscious about the depletion of non-renewable resources, usage of renewable resources for power generation is essential. The use of solar energy for generation of electrical power is reliable due to its low operational cost compared to other modes of power generation. Solar power plants have a specific set of factors that scale down the operational efficiencies of solar panels. <sup>5</sup> Accumulation of dust on the solar panels is one of the major factors that decreases the efficiency of solar panels. Conventional cleaning methods used for cleaning of PV panels are often time consuming and tiresome as it involves manpower and availability only in late night and early morning hours. Although various other methods are already in existence to clean the solar panels, they lack proper monitoring facilities and are not cost effective. Hence, the development of a better cleaning robotic system considering the drawbacks of the earlier systems is very much essential. The present work aims at the design and fabrication of an economical and efficient cleaning robot for solar panels.

The design of the solar panel cleaning robot uses a microcontroller based automatic cleaning action. While developing the model of the robot size, weight, mechanical stability, cost, cleaning methodology are considered. The model has three rotating brushes aligned across the body of the panel and are driven by three DC geared motors. A horizontal brush is placed behind the circular brushes for wet cleaning for more effective cleaning of the solar panels. The linear actuation system is implemented with the help of wheels attached to the shaft of heavy duty DC geared motors. Also, a 3D model of the robot is developed using software called SolidWorks.

#### 6.1 Conclusion

Based on the dust analysis performed, the following has been concluded:

- The efficiency of the panel reduces due to the accumulation of dust. Hence a solar panel cleaning robot has been designed and fabricated.

- As there are three rotating brushes and one rectangular brush for cleaning of the panel, the entire surface of the solar panel is covered while cleaning.
- The wet brush behind the row of rotating brushes carry out the cleaning further with water. If any amount of dust is left uncleaned, it is cleaned by the wet brushes.
- As a separate docking system is designed on the side of the panel to charge the robot, the overall weight of the cleaning robot is decreased. This reduces the chances of damaging the panel.
- The weight of the model is around 20-25 kg.
- The cost of the developed cleaning robot is less than the other cleaning systems.

## 6.2 Future Scope

The following are the future scope of the project:

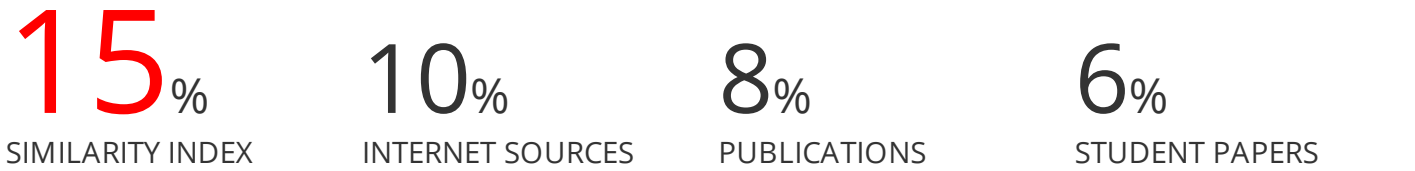
- The intelligent system with application of image processing algorithms can be introduced to estimate the amount of dust on the panel.
- Dust analysis can be performed using current, voltage and dust sensors and the real time data can be analyzed through cloud.
- A compact small size robot that can be built for small scale installations.

## 6.3 Learning Outcomes

- Knowledge of solar energy and its prominence in today's world.
- Understanding the design of various electrical motors.
- Programming microcontrollers.
- Knowledge of IoT.

# Design and Fabrication of Solar PV Cleaning Robot

## ORIGINALITY REPORT



## PRIMARY SOURCES

- | Rank | Source   | Percentage |
|------|--|------------|
| 1    | V. Chayapathy, G S Anitha, B Sharath. "IOT based home automation by using personal assistant", 2017 International Conference On Smart Technologies For Smart Nation (SmartTechCon), 2017<br>Publication  | 2%         |
| 2    | <a href="http://www.researchgate.net">www.researchgate.net</a><br>Internet Source  | 1 %        |
| 3    | <a href="http://ieeexplore.ieee.org">ieeexplore.ieee.org</a><br>Internet Source  | 1 %        |
| 4    | <a href="http://www.lib.utexas.edu">www.lib.utexas.edu</a><br>Internet Source  | 1 %        |
| 5    | G. Aravind, Gautham Vasan, T.S.B. Gowtham Kumar, R. Naresh Balaji, G. Saravana Ilango. "A Control Strategy for an Autonomous Robotic Vacuum Cleaner for Solar Panels", 2014 Texas Instruments India Educators' Conference (TIIEC), 2014<br>Publication | 1 %        |
| 6    | <a href="http://lib.buet.ac.bd:8080">lib.buet.ac.bd:8080</a><br>Internet Source  | 1 %        |

---

7	dergipark.ulakbim.gov.tr Internet Source	<1 %
8	Submitted to Universiti Teknologi Malaysia Student Paper	<1 %
9	Submitted to Universiti Putra Malaysia Student Paper	<1 %
10	www.thomasnet.com Internet Source	<1 %
11	Submitted to Higher Education Commission Pakistan Student Paper	<1 %
12	docs.neu.edu.tr Internet Source	<1 %
13	www.energysage.com Internet Source	<1 %
14	Jinxin Chen, Guobing Pan, Jing Ouyang, Jin Ma, Lei Fu, Libin Zhang. "Study on impacts of dust accumulation and rainfall on PV power reduction in East China", Energy, 2020 Publication	<1 %
15	Alireza Gheitasi, Ali Almaliky, Nawaf Albaqawi. "Development of an automatic cleaning system for photovoltaic plants", 2015 IEEE PES Asia-Pacific Power and Energy Engineering Conference (APPEEC), 2015 Publication	<1 %

---

16	Submitted to Visvesvaraya Technological University, Belagavi Student Paper	<1 %
17	www.igi-global.com Internet Source	<1 %
18	Submitted to Loughborough University Student Paper	<1 %
19	rees52.com Internet Source	<1 %
20	dokumen.pub Internet Source	<1 %
21	www.solarreviews.com Internet Source	<1 %
22	www.dekmake.com Internet Source	<1 %
23	Submitted to Universiti Teknologi MARA Student Paper	<1 %
24	archive.org Internet Source	<1 %
25	Submitted to University of Alabama Student Paper	<1 %
26	tudr.thapar.edu:8080 Internet Source	<1 %
27	Submitted to Asian Institute of Technology	

- 
- 28 Submitted to Federal University of Technology <1 %  
Student Paper
- 29 Submitted to Swinburne University of Technology <1 %  
Student Paper
- 30 www.researchpublish.com <1 %  
Internet Source
- 31 Submitted to University College Technology Sarawak <1 %  
Student Paper
- 32 Submitted to University of Northumbria at Newcastle <1 %  
Student Paper
- 33 Vikas Singh Panwar, Anish Pandey, Md. Ehtesham Hasan. "Design and fabrication of a novel concept-based autonomous controlled solar powered four-wheeled Floor Cleaning Robot for wet and dry surfaces", International Journal of Information Technology, 2022 <1 %  
Publication
- 34 repository.ntu.edu.sg <1 %  
Internet Source
- 35 Submitted to CSU, Stanislaus <1 %  
Student Paper

36	pdfcoffee.com Internet Source	<1 %
37	www.xcluma.com Internet Source	<1 %
38	1library.net Internet Source	<1 %
39	Submitted to University of Nottingham Student Paper	<1 %
40	researchspace.ukzn.ac.za Internet Source	<1 %
41	Submitted to American University of the Middle East Student Paper	<1 %
42	Submitted to Piri Reis University Student Paper	<1 %
43	Submitted to Universiti Teknikal Malaysia Melaka Student Paper	<1 %
44	Submitted to Universiti Tenaga Nasional Student Paper	<1 %
45	WWW.GABRIAN.COM Internet Source	<1 %
46	cyberleninka.org Internet Source	<1 %

47	res.mdpi.com Internet Source	<1 %
48	Submitted to Postgraduate Institute of Medicine Student Paper	<1 %
49	Submitted to Sim University Student Paper	<1 %
50	iopscience.iop.org Internet Source	<1 %
51	vdoc.pub Internet Source	<1 %
52	www.coursehero.com Internet Source	<1 %
53	hobohome.com Internet Source	<1 %
54	repository.asu.edu Internet Source	<1 %
55	www.jetir.org Internet Source	<1 %
56	Submitted to British University in Egypt Student Paper	<1 %
57	iferpjurnal.org Internet Source	<1 %
58	www.electricaltechnology.org	

Internet Source

<1 %

59

[www.sustainable.co.za](http://www.sustainable.co.za)

<1 %

60

"The Art of Modeling Mechanical Systems",  
Springer Science and Business Media LLC,  
2017

<1 %

Publication

61

Armin Barghi, Amir Reza Kosari, Maede Shokri, Samad Sheikhaei. "Intelligent lighting control with LEDS for smart home", 2014  
Smart Grid Conference (SGC), 2014

<1 %

Publication

62

COMPEL: The International Journal for Computation and Mathematics in Electrical and Electronic Engineering, Volume 33, Issue 4 (2014-09-16)

<1 %

Publication

63

Saed Tarapiah, Shadi Atalla. "Public Transportation Management System based on GPSWiFi and Open Street Maps", International Journal of Advanced Computer Science and Applications, 2015

<1 %

Publication

64

[doczz.fr](http://doczz.fr)

<1 %

Internet Source

ir.msu.ac.zw:8080

65

&lt;1 %

66

[repository.najah.edu](http://repository.najah.edu)

Internet Source

&lt;1 %

67

[tuprints.ulb.tu-darmstadt.de](http://tuprints.ulb.tu-darmstadt.de)

Internet Source

&lt;1 %

68

[www.technophiles.com](http://www.technophiles.com)

Internet Source

&lt;1 %

69

Mohammad Reza Maghami, Hashim Hizam, Chandima Gomes, Mohd Amran Radzi, Mohammad Ismael Rezadad, Shahrooz Hajighorbani. "Power loss due to soiling on solar panel: A review", Renewable and Sustainable Energy Reviews, 2016

Publication

&lt;1 %

70

Mohammad A. Jaradat, Mohammad Tauseef, Yousuf Altaf, Roba Saab, Hussam Adel, Nadeem Yousuf, Yousef H. Zurigat. "A fully portable robot system for cleaning solar panels", 2015 10th International Symposium on Mechatronics and its Applications (ISMA), 2015

Publication

&lt;1 %

Exclude bibliography Off